NASA CONTRACTOR REPORT

NASA CR-1479

RESEARCH AND DEVELOPMENT PROGRAM ON ORBITRON ULTRAHIGH VACUUM GAUGE

by F. J. Brock

Prepared by
NORTON RESEARCH CORPORATION
Cambridge, Mass.
for Langley Research Center

NATIONAL AERONAUTICS AND SPACE ADMINISTRATION • WASHINGTON, D. C. • DECEMBER 1969

RESEARCH AND DEVELOPMENT PROGRAM ON ORBITRON ULTRAHIGH VACUUM GAUGE

By F. J. Brock

Prepared under Contract No. NAS 1-5347, Task 7 by
NORTON RESEARCH CORPORATION
Cambridge, Mass.

for Langley Research Center

NATIONAL AERONAUTICS AND SPACE ADMINISTRATION

For sale by the Clearinghouse for Federal Scientific and Technical Information
Springfield, Virginia 22151 – Price $3.00

ABSTRACT

Mathematical procedures are outlined to obtain a self-consistent solution for the space charge dependent potential distribution of the orbitron gage. A computer program was used to obtain a set of geometric and electrical parameters for developing an orbitron gage.

TABLE OF CONTENTS

LIST OF FIGURES

LIST OF TABLES

RESEARCH AND DEVELOPMENT PROGRAM ON ORBITRON ULTRAHIGH VACUUM GAUGE

By F. J. Brock

Norton Research Corporation

SUMMARY

The previously developed orbitron theory was reformulated mathematically, such that it is amenable to machine solution. A computer program was written and all subroutines, functions, and operations tested The Fortran source code directs the machine to produce self-consistent solutions for the space charge dependent potential distribution, space charge density distribution, and the functional inverse of the electron radial position as a function of time, for an arbitrary set of prescribed input parameters consisting of geometrical parameters and the ratio of orbit injection kinetic energy to anode voltage. The program is written for an arbitrary number of iterations with continuous testing for convergence and orbit stability. The program also calculates many interesting parameters, such as orbit period, stability parameter, value of the electron Hamiltonian, electron average velocity, total number of electrons in the rotating space charge cloud and the ion production rate

The program was used to obtain several families of convergent, self-consistent solutions in a parameter survey with the value of the electron Hamiltonian taken as family parameter. A machine experiment was conducted, the results of which strongly imply that the solutions obtained are unique.

The conditions of optimum charge storage and ion production rate for each family of solutions are obvious from the results obtained. It is concluded from the solutions obtained that a relatively high total charge may be stored stably in the orbitron rotating electron cloud, and therefore relatively high ion production rates may be obtained.

INTRODUCTION

In a previous report (ref. 1), the orbitron principle, the orbitron electrical and geometrical configurations and the rotating electron cloud configuration and behavior were discussed in some detail; and a mathematical procedure was outlined for obtaining a self-consistent solution for the space charge dependent potential distribution and a 1st iteration approximate solution was worked out. Subsequently, the mathematical procedure for obtaining a self-consistent solution of the orbitron problem by numerical, iterative techniques has been developed more completely. Machine programs have been written, tested, and used to obtain many self-consistent orbitron solutions for a range of geometrical, electrical, and electron injection parameters.

The mathematical procedure used in this work is fundamentally that previously outlined, however the analysis has been reformulated to facilitate translation into machine language; and in minimizing the computer time required to obtain a convergent solution, it was found necessary to introduce several major modifications in the procedure; also the mathematical formulation has been further developed and is now essentially complete For these reasons, and to provide an intelligable transition from the analytical results

to the computer program and the numerical results, it is considered necessary to present the mathematical formulation in its entirety, even though this unavoidably leads to some repitition of previously presented material.

The orbitron consists of two coaxial cylinders, between which is applied a potential difference which produces a logarithmic potential distribution within the interelectrode space and a central force field which is attractive for electrons. An electron stream is injected into the interelectrode space with injection parameters such that the electrons execute open, ellipse-like, stable trajectories in the (r,θ) plane while drifting in the z-direction. Auxiliary electrodes at the ends of the cylinders produce mirror fields which reflect the electrons such that they oscillate along the z-axis.

It is assumed that the charge density is entirely eletronic; that the length of the cylindrical electrode assumbly is sufficiently large compared to its diameter that end effects may be neglected and that the charge density distribution is uniform along the z-axis; that the charge density distribution is uniform in the θ-direction (that injection parameters resulting in nonuniform, stationary charge distributions in the θ direction are disallowed); and that electrons are injected into stable, bound trajectories, only (that injection parameters outside the stable trajectory range are disallowed).

Under these assumptions, the Poisson equation and the continuity equation become ordinary differential equations in one dimension, r.

SELF-CONSISTENT ORBITRON THEORY

The rotating electron cloud which exists in the interelectrode space has an outer boundry which coincides with the

outer turning point of the electron trajectory The electron cloud obviously occupies only a part of the interelectrode space. It is mathematically convenient (but with no loss of generality) to assume that the electrons are injected into orbit at the outer turning point and that the injection angle (angle between the radius vector and velocity vector) is $\pi/2$. It turns out, physically, that these values are also the most convenient values of these two injection parameters. The injection parameter set is thus reduced to one free parameter the angular momentum

To provide for geometrical and electrical scaling of the machine results it is necessary to convert the radial coordinate and potential distribution to dimensionless variables. In the following treatment this is done by normalizing the radial coordinates with respect to r_o , the value of r at the outer turning point of the electron trajectory, and by normalizing the potential distribution with respect to V , the anode potential. Thus the dimensionless radial coordinate is $x \equiv r/r_o$ and the dimensionless potential distribution is $\phi(x) \equiv \Phi(r/r_o)/V$.

Potential Distribution

Developing a self-consistent solution for the space charge dependent potential distribution requires the simultaneous solution of the system of differential equations and applicable boundary conditions which describe the potential distribution as a function of the space charge density distribution, the space charge density distribution as a function of the radial component of the electron velocity, and the radial component of the electron velocity as a function of the space charge dependent potential distribution, but constrained such that only stable trajectories are allowed.

Since the rotating electron cloud occupies only a thick cylindrical region coaxial with the electrode assembly cylindrical axis of symmetry such that there is a space charge free region between the anode and the inner boundry of the electron cloud and a space charge free region between the outer boundary of the electron cloud and the outer cylindrical electrode, the Poisson equation must be applied to each region separately and then the three solutions matched at their boundaries.

Figure 1 is a schematic of the orbitron, applicable to the space charge dependent potential distribution problem. The curve $\phi(x)\big|_{\rho=0}$ is the space charge free potential distribution. The curve ϕ_ρ is the modification to the potential distribution introduced by inserting the space charge distribution $\rho(x)$. The self-consistent space charge dependent potential distribution is thus the sum of these two components, provided that the space charge density distribution is that which results from the same potential distribution.

There the self-consistent, space charge dependent potential distribution must satisfy the following system of differential equations, matching equations, and boundary equations:

$$\frac{1}{x}\frac{d}{dx}\left\{x\,\frac{d\phi_1(x)}{dx}\right\} = 0\ , \quad x_i \le x \le x_i\ , \tag{1}$$

$$\frac{1}{x}\frac{d}{dx}\left\{x\,\frac{d\phi_2(x)}{dx}\right\} = -\frac{r_o^{\,2}\rho(x)}{\varepsilon}\ , \quad x_i \le x \le 1\ , \tag{2}$$

$$\frac{1}{x}\frac{d}{dx}\left\{x\,\frac{d\phi_3(x)}{dx}\right\} = 0\ , \quad 1 \le x \le X_o \tag{3}$$

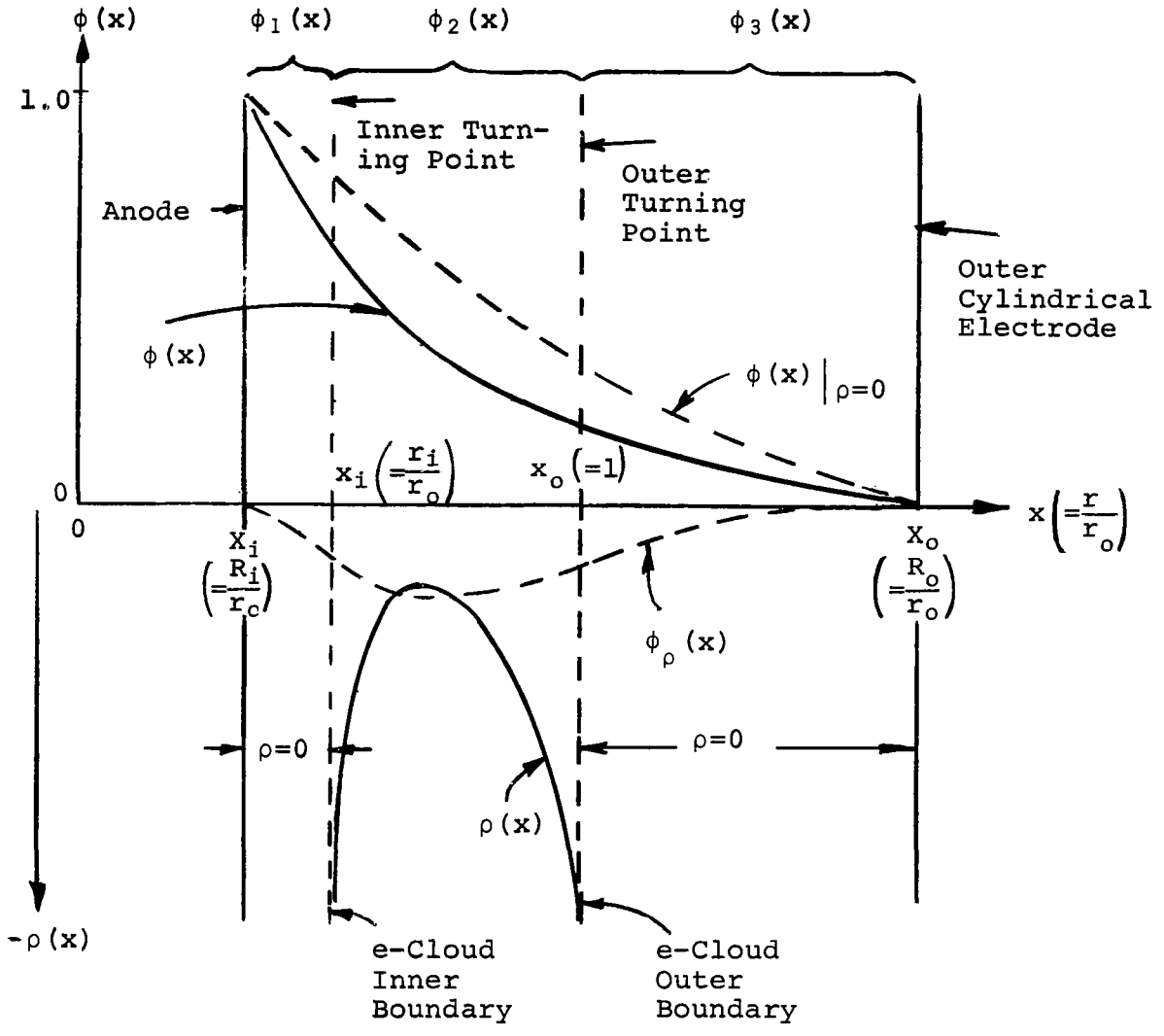

Fig. 1

Orbitron Potential Diagram (Schematic)

$$\phi_1(x_i) = \phi_2(x_i) \ , \tag{4}$$

$$\left.\frac{d\phi_1(x)}{dx}\right|_{x_i} = \left.\frac{d\phi_2(x)}{dx}\right|_{x_i} \ , \tag{5}$$

$$\phi_2(1) = \phi_3(1) \ , \tag{6}$$

$$\left.\frac{d\phi_2(x)}{dx}\right|_{x=1} = \left.\frac{d\phi_3(x)}{dx}\right|_{x=1} \ , \tag{7}$$

$$\phi_1(X_i) = 1 \ , \tag{8}$$

and

$$\phi_3(X_o) = 0 \ . \tag{9}$$

Suppose the total number of electrons in unit length (measured along the z-axis) of the rotating electron cloud is N_L , then

$$2\pi \int_{x_i}^{1} r_o^2 \rho(x) x dx = -eN_L \ . \tag{10}$$

It is convenient and useful (later in the computer program) to define the dimensionless charge integral $g(x)$ such that

$$\int_{x_i}^{x} r_o^2 \rho(x')x'dx' = - \frac{eN_L}{2\pi} g(x) \quad . \tag{11}$$

It is clear that

$$g(x_i) = 0 \tag{12}$$

and

$$g(1) = 1 \quad . \tag{13}$$

Similarly, the 2nd integral over the charge density may be defined as $h(x)$, such that

$$\int_{x_i}^{x} \frac{dx'}{x'} \int_{x_i}^{x'} r_o^2 \rho(x'')x''dx'' = - \frac{eN_L}{2\pi} \int_{x_i}^{x} g(x')\frac{dx'}{x'} \equiv - \frac{eN_L}{2\pi} h(x) \quad . \tag{14}$$

$h(x)$ is also dimensionless and it is clear that

$$h(x_i) = 0 \quad , \tag{15}$$

and using the mean value theorem and Eq. (13) it follows that (ref. 2)

$$h(1) \leq \log\left(\frac{1}{x_i}\right) , \tag{16}$$

for physically realizable electronic charge density distributions. It is also convenient to define the dimensionless parameter

$$Q \equiv \frac{eN_L}{2\pi\varepsilon V} , \tag{17}$$

where $V \equiv$ anode voltage (assuming the outer cylinder voltage is zero).

The solution to the system, Eq. (1) thru Eq. (9), for an arbitrary charge density distribution, is

$$\phi_1(x) = \frac{\log\frac{X_o}{x}}{\log\frac{X_o}{X_i}} - Q\left\{\log X_o + h(1)\right\}\frac{\log\frac{x}{x_i}}{\log\frac{X_o}{X_i}} , \quad X_i \leq x \leq x_i , \tag{18}$$

$$\phi_2(x) = \frac{\log\frac{X_o}{x}}{\log\frac{X_o}{X_i}} - Q\left\{\left[\log X_o + h(1)\right]\frac{\log\frac{x}{X_i}}{\log\frac{X_o}{X_i}} - h(x)\right\} , \quad x_i \leq x \leq 1 , \tag{19}$$

$$\phi_3(x) = \frac{\log\frac{X_o}{x}}{\log\frac{X_o}{X_i}} - Q\left\{\log\frac{1}{X_i} - h(1)\right\}\frac{\log\frac{X_o}{x}}{\log\frac{X_o}{X_i}} , \quad 1 \leq x \leq X_o . \tag{20}$$

Charge Density Distribution

The charge density distribution may be derived from statistical reasoning. Consider the motion of a single electron along its trajectory s. The fraction of the orbit period during which the electron is in the infinitesimal interval ds is dt/τ, where τ is the orbit period and dt is the infinitesimal interval of time, considered a function of s, that the electron spends in ds. The position probability distribution of the electron, $\psi(s)$, is the fraction of the period spent in ds per unit length along the trajectory, that is

$$\psi(s) = \frac{dt}{\tau ds} = \frac{1}{\tau}\frac{1}{v(s)} . \tag{21}$$

The increment of electronic charge that may be associated with the trajectory increment ds is therefore

$$dQ_e(s) = - e\ \psi(s)ds . \tag{22}$$

Referring to Fig. 2, the increment of charged contained in the cylindrical volume between r and $r + dr$ and length L (sufficiently large to contain the entire trajectory, is

$$dQ_e(r) = \rho_e(r)dV = L\ \rho_e(r)2\pi r dr , \tag{23}$$

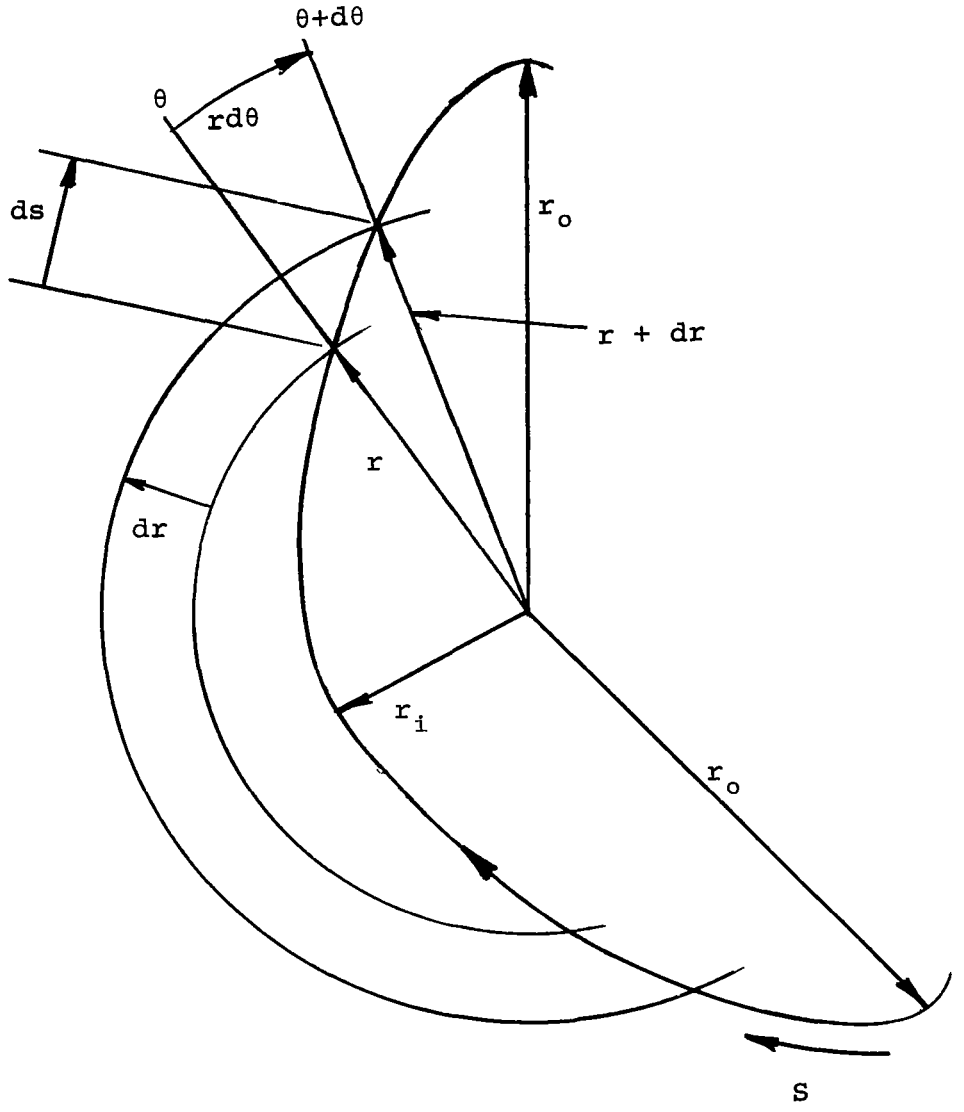

Fig. 2

where $\rho_e(r)$ is the mean charge density, considered a function of r, associated with a single orbiting electron. Since the trajectory passes twice thru the volume element it is clear that $dQ_e(r) = 2dQ_e(s)$ and since $ds = \left[1 + (d\theta/dr)^2\right]^{\frac{1}{2}}dr$ and $v(s) = \left[1 = (d\theta/dt)^2(dt/dr)^2\right]^{\frac{1}{2}} \overset{\circ}{r}$, it follows that

$$\left\{\pi L\rho_e(r)r + \frac{e}{\tau \overset{\circ}{r}(r)}\right\} dr = 0 \ , \tag{24}$$

where $\overset{\circ}{r}(r)$ is the radial component of the electron velocity. Therefore the mean charge density associated with one electron is

$$\rho_e(r) = - \frac{e}{\pi L\tau} \frac{1}{r\overset{\circ}{r}(r)} \ , \tag{25}$$

and the charge density distribution resulting from N_L electrons per unit length is

$$\rho(r) = - \frac{eN_L}{\pi\tau} \frac{1}{r\overset{\circ}{r}(r)} \ , \tag{26}$$

and written in terms of the dimensionless coordinate x, the charge density for an arbitrary radial velocity component is

$$\rho(x) = - \frac{eN_L}{\pi\tau r_o} \frac{1}{x\dot{r}(x)} , \tag{27}$$

where

$$\tau = 2r_o \int_{x_i}^{1} \frac{dx}{\dot{r}(x)} . \tag{28}$$

Electron Trajectory

The radial component of the electron velocity must satisfy the system

$$m(\ddot{r} - r\dot{\theta}^2) = e \frac{d\Phi_2(r)}{dr} , \tag{29}$$

and

$$\frac{d}{dr} \left\{ mr^2\dot{\theta} \right\} = 0 . \tag{30}$$

Eq. (30) has the solution

$$\dot{\theta} = \frac{\ell}{mr^2} , \tag{31}$$

where ℓ is the electron orbital angular momentum which may be expressed in terms of the electron kinetic energy at the outer turning point $T(r_o)$, by the equation

$$\ell^2 = 2mr_o^2 T(r_o) \ . \tag{32}$$

Substituting Eq. (31) and Eq. (32) into Eq. (29), integrating, and applying the boundry condition

$$\dot{r}(r_o) = 0 \ , \tag{33}$$

gives the radial component of the electron velocity

$$\left\{\dot{r}(r)\right\}^2 = \frac{2e}{m}\left\{\Phi_2(r) - \Phi_2(r_o)\right\} - \frac{2T}{m}(r_o)\left\{\frac{r_o^2}{r^2} - 1\right\} \ . \tag{34}$$

It is convenient to introduce the dimensionless kinetic energy, defined as

$$T \equiv \frac{T(r_o)}{ev} \ . \tag{35}$$

The radial component of the electron velocity, for an arbitrary potential distribution, written in terms of the dimensionless coordinate x is given by

$$\dot{r}(x) = \left(\frac{2ev}{m}\right)^{\frac{1}{2}} \left\{\phi_2(x) - \phi_2(1) - T(x^{-2} - 1)\right\}^{\frac{1}{2}} . \qquad (36)$$

Integrating Eq. (36) with respect to x gives the functional inverse of the trajectory, $t(x)$. Thus

$$\frac{t(x)}{\tau_{\frac{1}{2}}} = \frac{\displaystyle\int_{x_i}^{x} \left\{\phi_2(x') - \phi_2(1) - T\left[(x')^{-2} - 1\right]\right\}^{-\frac{1}{2}} dx'}{\displaystyle\int_{x_i}^{1} \left\{\phi_2(x) - \phi_2(1) - T(x^{-2} - 1)\right\}^{-\frac{1}{2}} dx} . \qquad (37)$$

where $\tau_{\frac{1}{2}} \equiv$ half-period is obtained from Eq. (28), and $t = 0$ has been taken to coincide with the inner turning point.

Observing that

$$\frac{1}{r_o} \frac{d\theta}{dx} = \frac{\dot{\theta}}{\dot{r}} , \qquad (38)$$

Eqs. (31) and (36) may be used to obtain θ as a function of x. Thus

$$\frac{d\theta}{dx} = \frac{T^{\frac{1}{2}}}{x^2} \left\{\phi_2(x) - \phi_2(1) - T(x^{-2} - 1)\right\}^{-\frac{1}{2}} , \qquad (39)$$

where Eq. (32) has been used to eliminate ℓ in favor of T. The azimuthal coordinate (as a function of x) is then given by

$$\frac{\theta(x)}{\Theta_{\frac{1}{2}}} = \frac{\int_{x_i}^{x} \left\{\phi_2(x') - \phi_2(1) - T\left[(x')^{-2} - 1\right]\right\}^{-\frac{1}{2}} \frac{dx'}{(x')^2}}{\int_{x_i}^{1} \left\{\phi_2(x) - \phi_2(1) - T(x^{-2} - 1)\right\}^{-\frac{1}{2}} \frac{dx}{x^2}} , \quad (40)$$

where $\Theta_{\frac{1}{2}} \equiv$ half-orbit angle, and $\theta = 0$ has been taken to coincide with the inner turning point.

Trajectory Stability

Orbital stability requires that the incremental force, resulting from an infinitesimal displacement of the electron from its trajectory by some perturbation interaction, must be directed such that it tends to restore the electron to its original trajectory, that is

$$df = - kdr , \quad (41)$$

where $k \equiv$ restoring force per unit displacement. Using Eq. (29), Eq. (31) and Eq. (32), the above equation may be evaluated in terms of the electric field and kinetic energy at the outer turning point, the least stable point in the electron trajectory,

$$df = d(m\ddot{r}) = -\left\{6T(r_o)\,\frac{r_o^2}{r^4} - e\,\frac{d^2\Phi_3(r)}{dr^2}\right\} dr \ . \qquad (42)$$

Orbital stability therefore requires

$$\left\{6T(r_o)\,\frac{r_o^2}{r^4} - e\,\frac{d^2\Phi_3(r)}{dr^2}\right\}\Bigg|_{r=r_o} > 0 \ . \qquad (43)$$

From the homogenious Poisson equation it follows

$$\frac{d^2\Phi_3(r)}{dr^2}\Bigg|_{r=r_o+} = -\frac{1}{r_o}\,\frac{d\Phi_3(r)}{dr}\Bigg|_{r=r_o} = \frac{-1}{r_o}\,\frac{d\Phi_3}{dr}(r)\Bigg|_{r=r_o} \ . \qquad (44)$$

Combining Eqs. (43) and (44), it follows that stable trajectories are those for which

$$T(r_o) > -\frac{er_o}{6}\,\frac{d\Phi_2}{dr}(r)\Bigg|_{r=r_o} \ . \qquad (45)$$

This is the outer turning point kinetic energy lower bound. The upper bound of the outer turning point kinetic energy is that associated with a circular trajectory having the same radius, thus

$$T(r_o) \leq - \frac{er_o}{2} \frac{d\Phi_2(r)}{dr}\bigg|_{r=r_o} . \tag{46}$$

It therefore follows that bound, stable electron trajectories are those for which

$$- \frac{er_o}{6} \frac{d\Phi_2(r)}{dr}\bigg|_{r=r_o} < T(r_o) \leq - \frac{er_o}{2} \frac{d\Phi_2(r)}{dr}\bigg|_{r=r_o} . \tag{47}$$

Eq. (47) may be written in a more useful form by differentiating Eq. (19), observing that $\frac{dh(x)}{dx} = \frac{g(x)}{x}$, evaluating the result at $r=r_o$ $(x = 1)$, applying Eq. (13), then substituting the result into Eq. (47), for the electric field, and finally applying Eq. (35), which gives

$$\frac{1}{3} < \frac{2T \log \frac{X_o}{X_i}}{1 - Q\left[\log \frac{1}{X_i} - h(1)\right]} \leq 1 . \tag{48}$$

It is convenient to introduce the dimensionless stability parameter α_s such that

$$\alpha_s = \frac{2T \log \frac{X_o}{X_i}}{1 - Q\left[\log \frac{1}{X_i} - h(1)\right]} , \tag{49}$$

which has the range, for stable, bound electron trajectories, given by

$$\frac{1}{3} < \alpha_s < 1 . \tag{50}$$

Eq. (49) is the orbital stability criterion and only those trajectories which satisfy this criterion are given further consideration.

Computational Procedure

In preparation for converting the results of the preceeding analysis to a computer program it is well to examine some of the ways that the computations necessary to produce a solution to the orbitron problem may be executed.

An immediately obvious procedure is to substitute for the radial component of the electron velocity $\overset{\circ}{r}(x)$, from Eq. (36) into the equation for the charge density distribution, $\rho(x)$ given by Eq. (27), and then substitute the result into the applicable Poisson equation, Eq. (2), which gives a differential equation for the charge dependant potential distribution

$$\frac{d}{dx}\left\{x\,\frac{d\phi_2(x)}{dx}\right\} = \left(\frac{eN_L}{2\pi\epsilon}\right)\frac{\left\{\phi_2(x) - \phi_2(1) - T(x^{-2} - 1)\right\}^{-\frac{1}{2}}}{\int_{x_i}^{1}\left\{\phi_2(x) - \phi_2(1) - T(x^{-2} - 1)\right\}^{-\frac{1}{2}}}\,, \quad (51)$$

in which $\frac{\tau}{2r_o}\left(\frac{2eV}{m}\right)^{\frac{1}{2}}$ has been eliminated by using Eqs. (28) and (36). It is, in general, more convenient to work with integral equations in computer computations rather than differential equations. Further, even if the starting function for $\phi_2(x)$ on the right in Eq. (51) were taken as the charge free potential distribution, the machine solution for $\phi_2(x)$ on the left would involve a double integration.

An alternative procedure which goes directly to the integral equation is to substitute for $r(x)$ from Eq. (36) into $\rho(x)$, Eq. (27), and then substitute the result into Eq. (19). This procedure gives the integral equation

$$\phi_2(x) = \frac{\log\frac{X_o}{x}}{\log\frac{X_o}{X_i}} - Q \log X_o \frac{\log\frac{x}{X_i}}{\log\frac{X_o}{X_i}}$$

$$- QG^{-1} \frac{\log\frac{x}{X_i}}{\log\frac{X_o}{X_i}} \int_{x_i}^{1} \frac{dx}{x} \int_{x_i}^{x} \left\{\phi_2(x') - \phi_2(1) - T\left[(x')^{-2} - 1\right]\right\}^{-\frac{1}{2}} dx'$$

$$+ QG^{-1} \int_{x_i}^{x} \frac{dx'}{x'} \int_{x_i}^{x'} \left\{\phi_2(x'') - \phi_2(1) - T\left[(x'')^{-2} - 1\right]\right\}^{-\frac{1}{2}} dx'' \qquad (52)$$

in which G has been evaluated using Eqs. (28) and (36)

$$G = \frac{\tau}{2r_o}\left(\frac{2eV}{m}\right)^{\frac{1}{2}} = \int_{x_i}^{1} \left\{\phi_2(x) - \phi_2(1) - T(x^{-2} - 1)\right\}^{-\frac{1}{2}} dx \ . \qquad (53)$$

This equation is compatable with conventional machine techniques and could, in fact, lead to a self-consistent solution for the space charge dependent potential distribution. However it imposes

an unnecessary computational burden on the machine and is therefore not an efficient procedure.

The only part of the self-consistent potential distribution which is unknown is the modification of the space charge free potential distribution resulting from insertion of the space charge. It will be shown below that this is principally dependent on $h(x)$. Therefore, a more efficient machine procedure is to substitute for $\overset{\circ}{r}(x)$ from Eq. (36) into $\rho(x)$, Eq. (27), and then substitute the result into Eq. (14) which gives the potential distribution modification resulting from the space charge more directly. The result of this arithmetic is

$$h(x) = G^{-1} \int_{x_i}^{x} \frac{dx'}{x'} \int_{x_i}^{x'} \left\{ \phi_2(x'') - \phi_2(1) - T\left[(x'')^{-2} - 1 \right] \right\}^{-\frac{1}{2}} dx'' \,, \qquad (54)$$

where G is obtained from Eq. (53).

For machine use, it is convenient to define a new dimentionless function $f(x)$, which is constructed from Eq. (36)

$$f(x) \equiv \left(\frac{2eV}{m} \right)^{\frac{1}{2}} \frac{1}{\overset{\circ}{r}(x)} = \left\{ \phi_2(x) - \phi_2(1) - T(x^{-2} - 1) \right\}^{-\frac{1}{2}} . \qquad (55)$$

$\phi_2(x)$ to be used in Eq. (55) must be taken from Eq. (19), thus

$\phi_2(x) - \phi_2(1) =$

$$\frac{\log\frac{1}{x}}{\log\frac{x_o}{x_i}} + Q\left[\log x_o + h(1)\right] \frac{\log\frac{1}{x}}{\log\frac{x_o}{x_i}} - Q\left[h(1) - h(x)\right] \quad . \tag{56}$$

$h(x)$ to be used in Eq. (56) is given by

$$h(x) = \int_{x_i}^{x} g(x') \frac{dx'}{x'} \quad , \tag{57}$$

where

$$g(x) = G^{-1} \int_{x_i}^{x} f(x')dx' \quad , \tag{58}$$

and

$$G = \int_{x_i}^{1} f(x)dx \quad . \tag{59}$$

The computational loop is now closed, $h(x)$ is generated from $f(x)$ which depends explicityly on $h(x)$, and if the system is convergent an iterative procedure may be used to obtain $h(x)$.

$\phi_2(x)$ is not only a function of $h(x)$ but also of Q, which in an iterative process must be regarded a variable parameter.

Q may be determined by recalling that the radial velocity goes to zero at the inner turning point

$$\dot{r}(x_i) = 0 \ , \tag{60}$$

or

$$f(x_i) = 0 \ . \tag{61}$$

Substituting Eq. (56) into Eq. (55) and the result into Eq. (61), evaluating at $x = x_i$, and solving for Q, gives

$$Q = \frac{T(x_i^{-2} - 1) \log\frac{X_o}{X_i} - \log\frac{1}{x_i}}{\log X_o \log\frac{1}{x_i} - h(1)\left[\log\frac{X_o}{X_i} - \log\frac{1}{x_i}\right]} \ . \tag{62}$$

It is obvious from this result that the only variable on which Q depends is $h(1)$, since T, x_i, X_i and X_o are considered prescribed parameters. T must however, be prescribed such that it satisfies the stability criterion, Eq. (49). The maximum value of T is associated with the maximum value of α_s. Indicating the maximum value of T by the subscript M and using Eq. (62) to eliminate Q, gives

$$T_M = \frac{\left[\log\frac{1}{x_i} - h(1)\right]}{2\left\{\log X_o \log\frac{1}{x_i} - h(1)\left[\log\frac{X_o}{X_i} - \log\frac{1}{x_i}\right]\right\} + (x_i^{-2} - 1)\left[\log\frac{1}{X_i} - h(1)\right]} \tag{63}$$

Therefore T must be prescribed such that

$$\frac{T_M}{3} < T \leq T_M \, , \tag{64}$$

for the electron trajectories to be stable.

The conditions for charge optimization may be studied by combining Eqs. (49) and (62) to eliminate T in terms of the stability parameter α_s, giving an expression for Q which depends only on directly prescribed parameters and the self-consistent solution for $h(x)\big|_{x=1}$. The result is

$$Q = \frac{\frac{\alpha_s}{2}\left(x_i^{-2} - 1\right) - \log\frac{1}{x_i}}{\log X_o \log\frac{1}{x_i} + \frac{\alpha_s}{2}(x_i^{-2} - 1)\log\frac{1}{X_i} - h(1)\left[\log\frac{X_o}{X_i} + \frac{\alpha_s}{2}(x_i^{-2} - 1) - \log\frac{1}{x_i}\right]} \tag{65}$$

All the parameters in Eq. (65) are independent except, of course, $h(1)$ which depends implicitly on x_i and α_s. Since $g(x)$ decreases everywhere except at the turning points as α_s increases, $h(1)$ decreases as α_s increases for fixed x_i. However the product $\alpha_s\, h(1)$ increases with α_s for fixed x_i. It thus turns out that the numerator of Eq. (65) increases faster than the denominator, from which it follows that Q increases with α_s for all other parameters fixed

The variation of Q with x_1 may be determined as follows: Since $h(1)$ is an implicit function of x_i (for α_s fixed), the mean value theorem may be applied to render the dependence explicit (at least in part). The integral expression for $h(1)$, Eq. (57), may then be written

$$h(1) = \int_{x_i}^{1} g(x)\,\frac{dx}{x} = g(\zeta)\int_{x_i}^{1}\frac{dx}{x} = g(\zeta)\log\frac{1}{x_i}\,, \tag{66}$$

in which ζ must be considered a function of x_i since x_i is now the only variable in the definition of $h(1)$, that is $\zeta = \zeta(x_i)$. Considering $\left[g\ \zeta(x_1)\right]$ to have only 2nd order dependence on x_i, to 1st order the dependence of $h(1)$ on x_i is given by $\log\frac{1}{x_1}$. Substituting Eq. (66) into Eq. (65) and taking the derivative of Q with respect to x_1 gives

$$\frac{dQ}{dx_i} < 0\,, \tag{67}$$

which implies that Q is a decreasing function of x_i. From this result it follows that the number of electrons per unit

length of the rotating space charge cloud is maximized (with respect to x_i) for x_i (the inner turning point) approaching X_i (the anode).

In some applications of the orbitron principle to practical devices it is important to know the value of the electron Hamiltonian. It is given by

$$H = T(r) - e\,\Phi_2(r) \quad , \tag{68}$$

and since H is a constant of motion it may be evaluated anywhere along the trajectory. It is convenient to evaluate it at the outer turning point, $r_o(x=1)$. Substituting from Eqs. (17), (19), (35) and (49) into Eq. (68) gives

$$\frac{H}{eV} = T\left[1 - \frac{\alpha_s}{2} \log X_o\right] \quad , \tag{69}$$

from which it is clear that the value of H depends only on the outer turning point kinetic energy, the stability parameter α_s, and X_o (the ratio of outer cylinder radius to outer turning point radius).

The computational procedure required to obtain a self-consistent solution for the space charge dependent potential distribution may now be outlined:

1.0 Prescribe X_i, x_i and X_o.

2.0 Initially, set $h(x) = h_o(x) = 0$.

3.0 Evaluate T_M using Eq. (63), ($h_o(1) = 0$ from 2.0 above),

4.0 Prescribe T .

5.0 Evaluate $Q_o = Q$ using Eq. (62), ($h_o(1) = 0$ from 2.0 above).

6.0 Perform J_{max} iterations ($J = 1, 2, \cdots J_{max}$) as follows:

6.1 Evaluate:

$$G_{J-1} = \int_{x_i}^{1} f_{J-1}(x)dx \ ;$$

take $f(x)$ from Eq. (55), and
$\phi_2(x) - \phi_2(1)$ from Eq. (56) in which $Q = Q_{J-1}$ but if $J-1 = 0$
take Q_o from 5.0 above, and
also in which $h(x) = h_{J-1}(x)$
but if $J-1 = 0$ take $h_o(x)$
from 2.0 above

6.2 Calculate and save (for all n ; $n=1, 2, \cdots n_{max}$)

$$g_{J-1}(x_n) = G_{J-1}^{-1} \int_{x_i}^{x_n} f_{J-1}(x)dx \ ;$$

take $f(x)$ as in 6 1 above,
note that $x_1 \equiv x_i$ and $x_{n_{max}} \equiv 1$

6.3 Calculate and save (for all n ; $n=1,2,\cdots n_{max}$:

$$h_J(x_n) = \int_{x_i}^{x_n} g_{J-1}(x_{n'}) \frac{dx_{n'}}{x_{n'}} ,$$

take $g_{J-1}(x_{n'})$ from 6.2 above,
note that $x_1 \equiv x_i$ and $x_{n_{max}} \equiv 1$.

6.4 Test $h_J(x_n)$ for convergence.

6.5 Evaluate Q_J from Eq. (62) using $h_J(1)$ from 6.3 above.

6.6 Evaluate α_{s_J} from Eq. (49) using $h_J(1)$ from 6.3 above and Q_J from 6.5 above.

6.7 Test α_{s_J} in Eq. (50); if satisfied, add 1 to J and return to 6.1. Repeat until $J = J_{max}$.

7.0 Plot the last computed values of the function $g_{J_{max}}(x_n)$ as a function of x_n for all n ; $n=1, 2,\cdots n_{max}$

8.0 Calculate $\phi_2(x_n)$ from Eq. (19) using $Q_{J_{max}}$ and $h_{J_{max}}(x_n)$ for all n ; $n=1, 2,\cdots n_{max}$

9.0 Plot the function $\phi_2(x_n)$ as a function of x_n for all n; $n=1, 2,\cdots n_{max}$.

10.0 Calculate ρ from Eqs. (27), (28), and (55)

$$- \frac{r_o^2 \rho(x_n)}{\varepsilon V} = \frac{Q_{J_{max}}}{G_{J_{max}}} \frac{f_{J_{max}}(x_n)}{x_n} .$$

11.0 Plot the function

$$\frac{Q_{J_{max}}}{G_{J_{max}}} \frac{f_{J_{max}}(x_n)}{x_n}$$

as a function of x_n for all n; n=1, 2,$\cdots n_{max}$.

12.0 Evaluate

$$\frac{\tau}{2r_o} \langle v \rangle = \int_{x_i}^{1} \left\{ 1 + \frac{T}{x^2} \left[f(x) \right]^2 \right\}^{\frac{1}{2}} dx$$

using $f_{J_{max}}(x)$.

Since $f(x)$ is unbounded at $x = x_i$ and $x = 1$, elementary machine integration routines do not yield precise values for the integral of $f(x)$, if the integration increment is constant, Δx_n = const. for all n Further an iteration procedure involving multiple integrations is not altogether compatable with the more sophisticated curve-fitting integration routines. It was therefore decided to use a variable increment, trapezoidal integration routine such that Δx is small where $\left|\frac{df}{dx}\right|$ is large and Δx is large where $\left|\frac{df}{dx}\right|$ is small. The integration increment is computed from

$$\Delta x_n = x_n - x_{n-1} ,$$

where

$$x_n = x_i + 2(1 - x_i) \sin^4\left\{\frac{\pi}{2} \frac{n}{n_{max}}\right\} ,$$

for

$$n \leq \frac{n_{max}}{2} ,$$

and

$$x_n = x_i + (1 - x_i)\left[1 - 2 \cos^4\left\{\frac{\pi}{2} \frac{n}{n_{max}}\right\}\right] ,$$

for

$$n > \frac{n_{max}}{2} .$$

The integration routine was tested by evaluating

$$\int_0^1 \frac{dx}{\left(\log\frac{1}{x}\right)^{\frac{1}{2}}} = \sqrt{\pi} ,$$

which diverges at $x = 1$ in a way which is similar to the divergence of $f(x)$ at $x = 1$. It was found that the value of

The above integral could be computed with adequate precision using about 500 integration increments, the machine results being a few parts in 10^5 less than the exact value.

Table I defines the computer source code symbols in terms of the symbols used in the analysis.

TABLE I

MACHINE PARAMETER	ANALYTIC PARAMETER
X , XF(N)	$X \quad \left(x = \frac{r}{r_o}\right)$
XI	$x_i \quad \left(x_i = \frac{r_i}{r_i}\right)$
1	$x_o \quad \left(x_o = 1\right)$
CXI	$X_i \quad \left(X_o = \frac{R_i}{r_o}\right)$
ALCXI	$\log X_i$
ALCXO	$\log X_o$
ALRCXI	$\log \frac{1}{X_i}$
ALCXOI	$\log \frac{X_o}{X_i}$
ALRXI	$\log \frac{1}{x_i}$

TABLE I (CONT.)

MACHINE PARAMETER	ANALYTIC PARAMETER
T	$T \left[T = \frac{T(r_o)}{eV} \right]$
Q	$Q \left[Q = \frac{eN_L}{2\pi\epsilon V} \right]$
A	α_s
GUMAX	$G \left[G = \int_{x_i}^{1} f(x)dx \right] = \left(\frac{2eV}{m} \right)^{\frac{1}{2}} \frac{1}{2r_o}$
GF(N)	$g(x) \left[g(x) = G^{-1} \int_{x_i}^{x} f(x')dx' \right]$ $\left[g(x) = \frac{t(x)}{\tau_{\frac{1}{2}}} \right]$
HF(N)	$h(x) \left[h(x) = \int_{x_i}^{x} g(x') \frac{dx'}{x'} \right]$
P	$\phi_2(x) \left[\phi_2(x) = \frac{\Phi_2(x)}{V} \right]$

TABLE I (CONT.)

MACHINE PARAMETER	ANALYTIC PARAMETER
RHO	$\frac{r_o^2 \rho(x)}{eV} \left[- \frac{r_o^2 \rho(r)}{eV} = QG^{-1} \frac{f(x)}{x} \right]$
RHOMN	$\left. \frac{r_o^2 \rho(x)}{eV} \right\|_{min}$
PXI	$\phi_2(x_i) \left[\phi_2(x_i) = \frac{\Phi(x_i)}{V} \right]$
PXO	$\phi_2(1) \left[\phi_2(1) = \frac{\Phi_2(1)}{V} \right]$
P/PØ)O	$\frac{\Phi_2(1)}{\left[V \frac{\log X_o}{X_o} \right]}$
N∘+L* (=[SVORDT][Q/GUMAX])	$\frac{\mathring{N}_L^+}{V^{3/2} n_g \sigma(\langle v \rangle) 2\pi\varepsilon \left[\frac{2}{em} \right]^{1/2}}$
<V>* (=SVORDT)	$\frac{\tau}{2r_o} \langle v \rangle$

The following computer program was written to perform the calculations outlined in the previous section. The program is written in Fortran for a time-shared machine (G.E. 265). The complete program, after compulation in binary machine code, is larger than the machine core. The program is therefore written in two parts: The first part of the program (ORB12), calculates the functions $g(x)$ and $h(x)$, executing a prescribed number of iterations. It also computes some other needed functions and evaluates a number of parameters, and executes a number of tests on the validity of the results. Some of these results are printed during program execution but most of the data are written on disc files prior to completion of the program. The second part of the program (ORB22), then continues the computations where the first part ended (it must be called manually). The second part of the program begins by reading the filed data back into the machine, plotting $g(x)$, then calculating and plotting $\rho(x)$ and $\phi_2(x)$ using the final $h(x)$ computed in the first part of the program. The data are plotted by a digital plotter, the resolution of which is 0.005 inches (California Computer Products, Model 210 Digital Plotting System) and which is driven by a GE265 time-shared computer.

ORB12

```
100 $FILE AL,XL1/XL2,GL1/GL2,HL1/HL2
110 DIMENSION XF(500),GF(500),HF(500)
120 PI=4.0*ATAN(1.0)
130 PIO2=2.0*ATAN(1.0)
140 200FORMAT(I3,1X,E15.9)
150 201FORMAT(I2,1X,E15.9)
160 202FORMAT(E15.9)
170 203FORMAT(I1)
180 204FORMAT(I3)
190 NMAX=500
200 YMAX=NMAX
210 JMAX=6
220 XI=0.388000
230 XO=1.0
240 CXI=0.380000
250 CXO=1.98500
260 XR=XO-XI
270 ALCXI=LOG(CXI)
280 ALCXO=LOG(CXO)
290 ALCXOI=LOG(CXO/CXI)
300 ALRCXI=LOG(1.0/CXI)
310 ALRXI=LOG(1.0/XI)
320 TMIN=1.0/(1.0/(XI*XI)-1.0)*ALRXI/ALCXOI
330 TMAX=1.0/((1.0/(XI*XI)-1.0)*ALRCXI/ALRXI+2.0*ALCXO)
340 PRINT202,TMIN,;PRINT," < T < ",;PRINT202,TMAX,;PRINT,"    T=",
350 INPUT,T
360 AQ=T*(1.0/(XI*XI)-1.0)*ALCXOI-ALRXI
370 IF(AQ)1,1,2
380 1PRINT,"AQ     =",;PRINT202,AQ
390 PRINT,"TRAJECTORY UNSTABLE"
400 GOTO98
410 2
420 Q=AQ/(ALCXO*ALRXI)
430 A1=(1.0+Q*ALCXO)/ALCXOI
440 PRINT,"NMAX   =",;PRINT204,NMAX
450 PRINT,"JMAX   =",;PRINT203,JMAX
460 PRINT,"XI     =",;PRINT202,XI
470 PRINT,"XO     =",;PRINT202,XO
480 PRINT,"CXI    =",;PRINT202,CXI
490 PRINT,"CXO    =",;PRINT202,CXO
500 PRINT,"T      =",;PRINT202,T
510 PRINT,"Q      =",;PRINT202,Q
520 PRINT,"A1     =",;PRINT202,A1
530 DO90J=1,JMAX
540 KS=1
550 KSQRT=0
560 PRINT,;"IN ITERATION ",;PRINT203,J
570 PRINT,
580 RFOS=A1*ALRXI-Q*HF(NMAX)-T*(1.0/(XI*XI)-1.0)
590 IF(RFOS)3,4,4
```

```
600 3
610 FO=1.0/SQRT(ABS(RFOS))
620 GOTO5
630 4FO=1.0/SQRT(RFOS)
640 5PRINT,"F(XI) =",;PRINT202,FO
650 DO30N=1,NMAX
660 Y=N
670 IF(J-1)98,6,14
680 6
690 S=SIN(PIO2*Y/YMAX)
700 C=COS(PIO2*Y/YMAX)
710 IF(N-NMAX/2)11,11,12
720 11X=XI+XR*(2.0)*S*S*S*S
730 GOTO13
740 12X=XI+XR*(1.0-2.0*C*C*C*C)
750 13XF(N)=X
760 14
770 RFS=A1*LOG(1.0/XF(N))-Q*(HF(NMAX)-HF(N))-T*(1.0/(XF(N)*XF(N))-1.0)
780 IF(RFS)15,16,16
790 15F=1.0/SQRT(ABS(RFS))
800 KSQRT=KSQRT+1
810 GOTO17
820 16F=1.0/SQRT(RFS)
830 17IF(N-1)98,21,22
840 21GU=(FO+F)*(XF(1)-XI)/2.0
850 GOTO26
860 22GU=GU+(FO+F)*(XF(N)-XF(N-1))/2.0
870 GOTO(23,26)KS
880 23IF(N-25)26,26,24
890 24IF(FO-F)25,25,26
900 25KS=2
910 FMIN=FO
920 NFMIN=N-1
930 RHOMIN=Q*FMIN/(GUMAX*XF(NFMIN))
940 26FO=F
950 GF(N)=GU
960 30
970 PRINT,"FMIN  =",;PRINT202,FMIN
980 PRINT,"NFMIN =",;PRINT204,NFMIN
990 GUMAX=GU
1000 PRINT,"F(XO) =",;PRINT202,FO
1010 PRINT,"GUMAX =",;PRINT202,GUMAX
1020 DO40N=1,NMAX
1030 DUMMY=GF(N)
1040 GF(N)=DUMMY/GUMAX
1050 40
1060 H=(GF(1)/XF(1))*(XF(1)-XI)/2.0
1070 HF(1)=H
1080 DHMAX=0.0
1090 DO60N=2,NMAX
```

```
1100 H=H+(GF(N)/XF(N)+GF(N-1)/XF(N-1))*(XF(N)-XF(N-1))/2.0
1110 DH=HF(N)-H
1120 IF(ABS(DH)-ABS(DHMAX))51,51,50
1130 50DHMAX=DH
1140 DELTA=DHMAX/(2.0*(H+HF(N)))
1150 NDHMAX=N
1160 51HF(N)=H
1170 60
1180 PRINT,"H(XO) =",;PRINT202,HF(NMAX)
1190 PRINT,"DELTA =",;PRINT202,DELTA
1200 PRINT,"NDHMAX=",;PRINT204,NDHMAX
1210 Q=AQ/(ALCXO*ALRXI+(ALRXI-ALCXOI)*HF(NMAX))
1220 A1=(1.0+Q*(ALCXO+HF(NMAX)))/ALCXOI
1230 A=(2.0*T*ALCXOI)/(1.0-Q*(ALRCXI-HF(NMAX)))
1240 PRINT,"KSQRT =",;PRINT203,KSQRT
1250 PRINT,"Q     =",;PRINT202,Q
1260 PRINT,"A1    =",;PRINT202,A1
1270 PRINT,"A     =",;PRINT202,A
1280 IF(1.0-A)70,71,71
1290 70PRINT,"TRAJECTORY UNBOUND"
1300 GOTO98
1310 71IF(A-(1.0/3.0))72,72,73
1320 72PRINT,"TRAJECTORY UNSTABLE"
1330 GOTO98
1340 73IF(J-JMAX)90,74,98
1350 74DO80N=1,NMAX
1360 VORDTS=1.0+T/(XF(N)*XF(N)*((1.0+Q*(ALCXO+HF(NMAX)))
1370 +*(LOG(1.0/XF(N))/ALCXOI)-Q*(HF(NMAX)-HF(N)))
1380 +-T*(1.0-XF(N)*XF(N)))
1390 VORDT=SQRT(ABS(VORDTS))
1400 IF(N-1)98,75,76
1410 75SVORDT=VORDT*(XF(1)-XI)
1420 GO1077
1430 76SVORDT=SVORDT+(VORDTO+VORDT)*(XF(N)-XF(N-1))/2.0
1440 77VORDTO=VORDT
1450 80
1460 90
1470 PRINT,↑↑↑"RHOMN*=",;PRINT202,RHOMIN
1480 PRINT,"<V>*  =",;PRINT202,SVORDT
1490 PXI=(ALCXO+ALRXI-Q*(ALCXO+HF(NMAX))*(ALRCXI-ALRXI))/ALCXOI
1500 PRINT,"PXI   =",;PRINT202,PXI
1510 PXO=(1.0-Q*(ALRCXI-HF(NMAX)))*(ALCXO/ALCXOI)
1520 PRINT,"PXO   =",;PRINT202,PXO
1530 PRINT,"P/P0)0=",;PRINT202,PXO*ALCXOI/ALCXO
1540 PRINT,"H/TXO =",;PRINT202,1.0-PXO/T
1550 PP1=SQRT(2.0*1.602E-19/9.11E-31)
1560 PRINT,"PP1   =",;PRINT202,PP1
1570 PP2=2.0*PI*8.85E-12/1.602E-19
1580 PRINT,"PP2   =",;PRINT202,PP2
1590 PRINT,"PP3   =",;PRINT202,PP1*PP2
```

ORB12 CONTINUED

```
1600 PRINT,"N.+L* =",;PRINT202,SVORDT*Q/GUMAX
1610 PRINT,"N.+L**=",;PRINT202,SVORDT*Q*PP1*PP2/GUMAX
1620 PRINT,"<V>** =",;PRINT202,SVORDT*PP1/GUMAX
1630 PRINT,"TAU** =",;PRINT202,2.0*GUMAX/PP1
1640 PRINT,"NL**  =",;PRINT202,Q*PP2
1650 WRITE(1,201)11,NMAX,12,JMAX,13,XI,14,CXI,15,CXO,16,TMIN,17,T,
1660 +18,TMIN,19,GUMAX,20,Q,21,A1,22,XR,23,ALCXI,24,ALCXO,25,ALCXOI,
1670 +26,ALRCXI,27,ALRXI,28,AQ,29,RHOMIN,30,SVORDT
1680 PRINT,"PARAMETERS WRITTEN ON FILE 1"
1690 WRITE(2,200)(100+N,XF(N),N=1,NMAX)
1700 PRINT,"XF(N) WRITTEN ON FILE 2"
1710 WRITE(4,200)(100+N,GF(N),N=1,NMAX)
1720 PRINT,"GF(N) WRITTEN ON FILE 4"
1730 WRITE(6,200)(100+N,HF(N),N=1,NMAX)
1740 PRINT,"HF(N) WRITTEN ON FILE 6"
1750 PRINT,↑↑"TO CONTINUE: CALL ORB2 (CHANGE TO PLO)"
1760 GOTO99
1770 98STOP"ERR"
1780 99
1790 $OPT TIME;$OPT SIZE
1800 END
```

ORB22

```
2000C     THIS PROGRAM PLOTS THE COORDINATE AXES FOR PHI(X),G(X),
2010C     AND RHO(X). IT IS WRITTEN FOR A 5 MILL PLOTTER DRIVEN BY
2020C     THE C-A-C GE265(NO CALL TO FACTOR).
2030C     IT READS THE FILES GENERATED BY ORB1 AND USES THIS DATA TO
2040C     PLOT OR CALCULATE AND PLOT PHI(X), G(X), AND RHO(X).
2050C     RHO(X) IS PLOTTED AS RHO/100.
2060C     THE PROGRAM MOVES THE PEN TO THE NEXT PAGE.
2070 $OPT PLOT
2080 $FILE AL,XL1/XL2,GL1/GL2,HL1/HL2
2090 DIMENSION XF(500),GF(500),HF(500)
2100 201FORMAT(I2,1X,E15.9)
2110 202FORMAT(E15.9)
2120 300FORMAT(3X,E15.9)
2130 301FORMAT(4X,E15.9)
2140 204FORMAT(I3)
2150 CALL PLOT(0.0,0.0,-3)
2160 CALL PLOT(12.0,0.0,2)
2170 X=12.0
2180 Y=0.0
```

ORB22 CONTINUED

```
2190 DO1M=1,11
2200 CALL PLOT(X,Y,3)
2210 CALL PLOT(X,Y+0.08,2)
2220 1X=X-1.2
2230 X=-0.16
2240 Y=0.16
2250 FPN=0.0
2260 DO2M=1,11
2270 CALL NUMBER(X,Y,0.16,FPN,0.0,2)
2280 X=X+1.2
2290 2FPN=FPN+0.1
2300 CALL PLOT(0.0,0.0,3)
2310 CALL PLOT(0.0,-16.0,2)
2320 X=0.0
2330 Y=-16.0
2340 DO3M=1,11
2350 CALL PLOT(X,Y,3)
2360 CALL PLOT(X-0.08,Y,2)
2370 3Y=Y+1.6
2380 X=-0.32
2390 Y=0.16
2400 FPN=0.0
2410 DO4M=1,11
2420 CALL NUMBER(X,Y,0.16,FPN,270.0,2)
2430 Y=Y-1.6
2440 4FPN=FPN+0.1
2450 CALL SYMBOL(-0.74,-7.90,0.30,"X",270.0,1)
2460 CALL PLOT(0.0,0.0,-3)
2470 1001PRINT,"START READ"
2480 READ(1,300)NMAX,JMAX,XI,CXI,CXO,W,T,W,GUMAX,Q,A1,XR,
2490 +ALCXI,ALCXO,ALCXOI,ALRCXI,ALRXI,AQ
2500 PRINT,"READ 1"
2510 READ(2,301)(XF(N),N=1,NMAX)
2520 PRINT,"READ 2"
2530 READ(4,301)(GF(N),N=1,NMAX)
2540 PRINT,"READ 4"
2550 READ(6,301)(HF(N),N=1,NMAX)
2560 PRINT,"READ 6"
2570 A2=ALCXO+HF(NMAX)
2580 DO20N=1,NMAX
2590 P=(ALCXO-LOG(XF(N)))/ALCXOI-Q*((A2/ALCXOI)*(LOG(XF(N))+ALRCXI)
2600 +-HF(N))
2610 X=(12.0)*P
2620 Y=(-16.000)*XF(N)
2630 CALL PLOT(X,Y,3)
2640 20CALL PLOT(X,Y,2)
2650 CALL PLOT(0.0,0.0,-3)
2660 DO70N=1,NMAX
2670 X=(12.0)*GF(N)
2680 Y=(-16.000)*XF(N)
```

ORB22 CONTINUED

```
2690 CALL PLOT(X,Y,3)
2700 CALL PLOT(X,Y,2)
2710 70
2720 CALL PLOT(0.0,0.0,-3)
2730 KT=0
2740 NMAXM5=NMAX-5
2750 DO95N=5,NMAXM5
2760 F1=Q*(HF(NMAX)-HF(N))
2770 F2=T*(1.0/(XF(N)*XF(N))-1.0)
2780 RFS=A1*LOG(1.0/XF(N))-F1-F2
2790 IF(RFS)75,76,76
2800 75F=1.0/SQRT(ABS(RFS))
2810 KT=KT+1
2820 GOTO80
2830 76F=1.0/SQRT(RFS)
2840 80RHO=Q*F/(GUMAX*XF(N))
2850 IF(RHO-10.0)90,90,95
2860 90X=(1.2)*RHO
2870 Y=(-16.000)*XF(N)
2880 CALL PLOT(X,Y,3)
2890 CALL PLOT(X,Y,2)
2900 95
2910 CALL PLOT(0.0,0.0,-3)
2920 CALL PLOT(18.75,0.0,-3)
2930 PRINT,"KT     =",;PRINT204,KT
2940 END
```

ORB3

```
3000 $OPT PLOT
3010 DIMENSION XI(7)
3020 CALL PLOT(0.0,0.0,-3)
3030 CALL PLOT(12.0,0.0,2)
3040 X=12.0
3050 Y=0.0
3060 DO1M=1,11
3070 CALL PLOT(X,Y,3)
3080 CALL PLOT(X,Y+0.08,2)
3090 1X=X-1.2
3100 X=-0.16
3110 Y=0.16
3120 FPN=0.0
3130 DO2M=1,11
```

ORB3 CONTINUED

```
3140 CALL NUMBER(X,Y,0.16,FPN,0.0,2)
3150 X=X+1.2
3160 2FPN=FPN+0.1
3170 CALL PLOT(0.0,0.0,3)
3180 CALL PLOT(0.0,-16.0,2)
3190 X=0.0
3200 Y=-16.0
3210 DO3M=1,11
3220 CALL PLOT(X,Y,3)
3230 CALL PLOT(X-0.08,Y,2)
3240 3Y=Y+1.6
3250 X=-0.32
3260 Y=0.16
3270 FPN=0.0
3280 DO4M=1,11
3290 CALL NUMBER(X,Y,0.16,FPN,270.0,2)
3300 Y=Y-1.6
3310 4FPN=FPN+0.1
3320 CALL SYMBOL(-0.74,-7.90,0.30,"XI",270.0,2)
3330 CALL PLOT(0.0,0.0,-3)
3340 NMAX=7
3350 DO15N=1,NMAX
3360 READ,XI(N)
3370 15
3380 DO20N=1,NMAX
3390 READ,T
3400 X=12.0*T
3410 Y=-16.0*XI(N)
3420 CALL PLOT(X,Y,3)
3425 CALL PLOT(X,Y,2)
3430 CALL SYMBOL(X,Y,0.13,"T",270.0,1)
3440 20
3450 CALL PLOT(0.0,0.0,-3)
3460 DO25N=1,NMAX
3470 READ,Q
3480 X=12.00*Q
3490 Y=-16.0*XI(N)
3500 CALL PLOT(X,Y,3)
3505 CALL PLOT(X,Y,2)
3510 CALL SYMBOL(X,Y,0.13,"Q",270.0,1)
3520 25
3530 CALL PLOT(0.0,0.0,-3)
3540 DO30N=1,NMAX
3550 READ,P
3560 X=12.0*P
3570 Y=-16.0*XI(N)
3580 CALL PLOT(X,Y,3)
3585 CALL PLOT(X,Y,2)
3590 CALL SYMBOL(X,Y,0.13,"P",270.0,1)
3600 30
```

```
3610 CALL PLOT(0.0,0.0,-3)
3620 DO35N=1,NMAX
3630 READ,AI
3640 X=12.0*AI
3650 Y=-16.0*XI(N)
3660 CALL PLOT(X,Y,3)
3665 CALL PLOT(X,Y,2)
3670 CALL SYMBOL(X,Y,0.13,"I+",270.0,2)
3680 35
3690 CALL PLOT(0.0,0.0,-3)
3700 DO40N=1,NMAX
3710 READ,R
3720 X=12.0*R
3730 Y=-16.0*XI(N)
3740 CALL PLOT(X,Y,3)
3745 CALL PLOT(X,Y,2)
3750 CALL SYMBOL(X,Y,0.13,"R",270.0,1)
3760 40
3770 CALL PLOT(0.0,0.0,-3)
3780 DO45N=1,NMAX
3790 READ,V
3800 X=12.0*V
3810 Y=-16.0*XI(N)
3820 CALL PLOT(X,Y,3)
3825 CALL PLOT(X,Y,2)
3830 CALL SYMBOL(X,Y,0.13,"V",270.0,1)
3840 45
3850 CALL PLOT(0.0,0.0,-3)
3860 DO50N=1,NMAX
3870 READ,G
3880 X=12.0*G
3890 Y=-16.0*XI(N)
3900 CALL PLOT(X,Y,3)
3905 CALL PLOT(X,Y,2)
3910 CALL SYMBOL(X,Y,0.13,"G",270.0,1)
3920 50
3930 CALL PLOT(0.0,0.0,-3)
3940 CALL PLOT(18.75,0.0,-3)
3950 END
3960 $DATA
3970 .100,.250,.388,.500,.600,.750,.900
3980 .009,.061,.147,.243,.350,.550,.790
3990 .476,.686,.795,.812,.775,.614,.309
4000 .059,.244,.433,.593,.725,.883,.978
4010 .133,.296,.441,.526,.563,.514,.287
4020 .082,.090,.105,.118,.131,.153,.177
4030 .125,.165,.203,.233,.260,.303,.360
4040 .446,.386,.367,.359,.359,.363,.386
```

In ORB12 a convergence test is performed on $h(x)$ during each iteration. This is done by computing the difference $h_{J-1}(x_n) - h_J(x_n)$ for all n, and then sorting out that value of n for which this difference has the largest absolute value The maximum relative difference between $h(x)$ generated in two successive iterations is then formed by computing

$$\Delta = \frac{\left| h_{J-1}(x_n) - h_J(x_n) \right|}{\frac{1}{2}\left| h_{J-1}(x_n) + h_J(x_n) \right|} ,$$

where n has the value determined above The value of n may change (and generally does) in each application of the above convergence test. However, it is found experimentally that the value of Δ is monotone decreasing if T satisfies the stability criterion It is also found that the rate of convergence (the decrease in Δ per iteration) depends on the value of T, within the stabile range (as well as on the other parameters), such that the rate of convergence increases as T decreases. This is to be expected since a decreasing T implies a decreasing Q. Δ and the value of n at which it is evaluated are printed during each iteration so that execution may be aborted if Δ does not approach zero.

It was found that Δ was within the range $10^{-6} < \Delta < 10^{-3}$ if T satisfied the stability criterion and at least 5 but not more than 10 iterations were executed. It appears that Δ may be made to approach the rounding error limit of the machine ($\sim 5 \times 10^{-8}$ for the GE 265) by performing a sufficiently large number of iterations. This was verified in a machine experiment in which, after 7 iterations, $\Delta < 10^{-7}$ and thereafter fluctuated, positive and negative, but such that $|\Delta| < 10^{-7}$ in all subsequent iterations.

The above tests for convergence of $h(x)$ still leaves open the question of uniqueness of the solution. That is, for the prescribed parameters is the final $h(x)$ the only $h(x)$ posible? A machine experiment was conducted in which the starting function, the initial $h_o(x)$, was varied over a wide range. It was found that the final $h_{J_{max}}(x)$ was the same function, $\Delta<10^{-7}$, ($\Delta \equiv$ relative difference between any two final $h_{J_{max}}(x)$) for all $h_o(x)$, completely independent of the definition of the initial $h_o(x)$. From these tests it is considered highly probable that all convergent solutions for $h(x)$ are unique.

RESULTS

An orbitron parameter survey was made in which all parameters, except x_i/X_i, were varied over most of their useful or allowed range, and convergent, self-consistent solutions for $h(x)$ were obtained for each set of parameters. The parameter x_i/X_i was not varied since it was shown in a previous section that Q was maximized with respect to x by setting $x_i/X_i = 1 + \delta$ where $\delta << 1$. This analytical result was however tested by obtaining a number of self-consistent solutions for a number of different values of x_i while holding all other prescribed parameters constant. The machine results verify the analytical conclusion, Eq. (67).

From the self-consistent solution for $h(x)$, the functions listed in Table II below, were computed and plotted. Since the curves are not all plotted to the same scale, the value of the ordinate applicable to each curve is also given in the table.

TABLE II

For Figs. 3 thru 9, Figs. 11 thru 17, and Figs. 19 thru 22.

CURVE LABLE	FUNCTION	ORDINATE FULL SCALE
G	$\equiv g(x) = \frac{t(x)}{\tau_{\frac{1}{2}}}$	1.0
ρ	$\equiv \frac{-r_o^2 \rho(x)}{eV} = \frac{Q}{G} \frac{f(x)}{x}$	10.0
ϕ	$\equiv \phi(x)$	1.0

The curves are plotted in dimensionless form. H (the electron Hamiltonian) was taken as family parameter and three sets of results are presented, corresponding to the following three values of H :

$$\frac{H}{T(r_o)} \propto \begin{cases} -0.4 \\ 0.0 \\ +0.55 \end{cases}$$

Following each of these three sets of graphs a summary of pertinent parameters is presented in graphical form. The parameters plotted in these summary graphs are listed in Table III.

TABLE III

For Figs. 10, 18, and 23

CURVE LABLE			ORDINATE FULL SCALE
T	$\equiv \frac{T(r_o)}{eV}$	Outer turning point kinetic energy	1.0
Q	$\equiv \frac{eN_L}{2\pi\epsilon V}$	$N_L \equiv$ Number of electrons per unit length	1.0
P	$\equiv \frac{\phi_2(1)}{\frac{\ln X_o}{\ln \frac{X_o}{X_i}}} = \left.\frac{\text{(space charge dependent potential)}}{\text{(charge free potential)}}\right\|_{\substack{r=r_o \\ (x=1)}}$		1.0
I+	$\equiv \frac{\tau}{2r_o}\langle v\rangle \frac{Q}{G}$	Ion production rate	1.0
	$= \frac{\dot{N}_L^+}{n_g\ \sigma(\langle v\rangle)\left(\frac{2\pi\epsilon V}{e}\right)\left(\frac{2eV}{m}\right)^{\frac{1}{2}}}$		
	($\dot{N}_L^+ \equiv$ number of ions produced per unit time)		
	($n_g \equiv$ gas number density)		
R	$\equiv -\left.\frac{r_o^2\rho(x)}{eV}\right\|_{min}$	minimum charge density	10.0
V	$\equiv \frac{\tau}{2r_o}\langle v\rangle$	mean velocity	10.0
G	$\equiv \left(\frac{2eV}{m}\right)^{\frac{1}{2}} \frac{\tau}{2r_o}$	orbit period	10.0

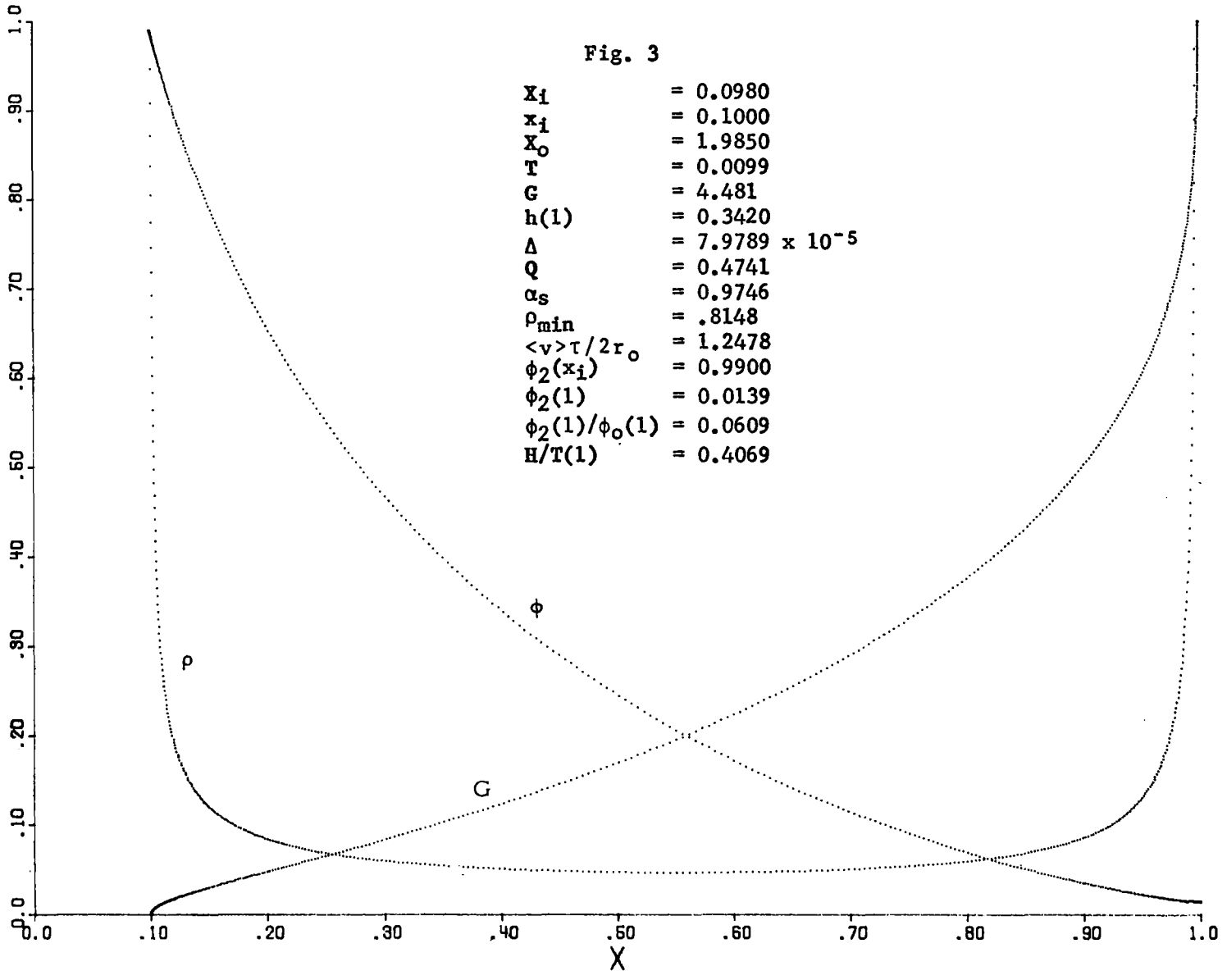
Fig. 3
X_i = 0.0980
x_i = 0.1000
X_o = 1.9850
T = 0.0099
G = 4.481
h(1) = 0.3420
Δ = 7.9789 x 10^{-5}
Q = 0.4741
α_s = 0.9746
ρ_{min} = .8148
$\langle v \rangle \tau / 2r_o$ = 1.2478
$\phi_2(x_i)$ = 0.9900
$\phi_2(1)$ = 0.0139
$\phi_2(1)/\phi_o(1)$ = 0.0609
H/T(1) = 0.4069
ρ
φ
G
0.0
.10
.20
.30
.40
.50
.60
.70
.80
.90
1.0
X

Fig. 4

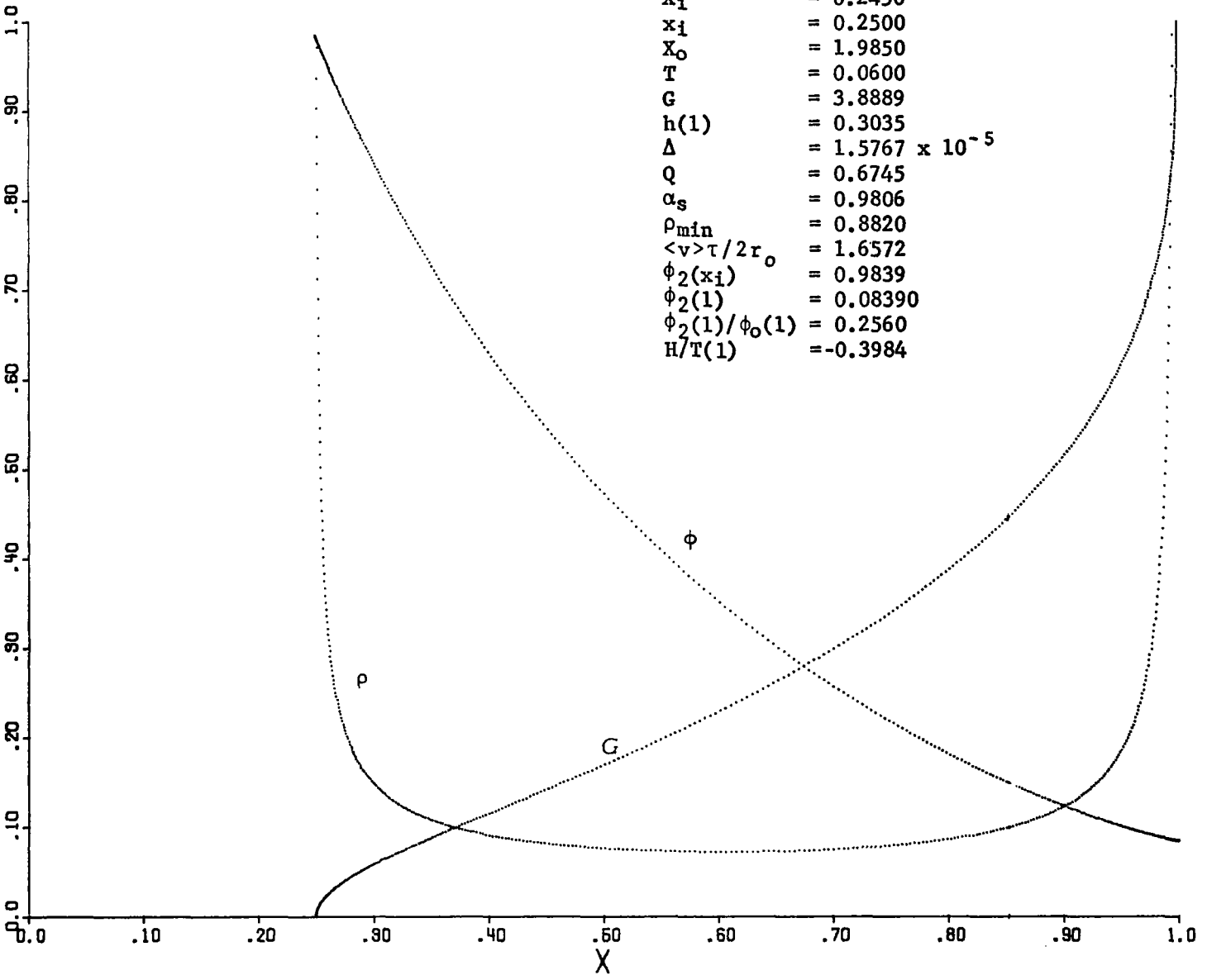
X_i = 0.2450
x_i = 0.2500
X_o = 1.9850
T = 0.0600
G = 3.8889
h(1) = 0.3035
Δ = 1.5767 x 10^{-5}
Q = 0.6745
α_s = 0.9806
ρ_{min} = 0.8820
$\langle v \rangle \tau / 2r_o$ = 1.6572
$\phi_2(x_i)$ = 0.9839
$\phi_2(1)$ = 0.08390
$\phi_2(1)/\phi_o(1)$ = 0.2560
H/T(1) = -0.3984
ϕ
ρ
G
0.0
.10
.20
.30
.40
.50
.60
.70
.80
.90
1.0
X

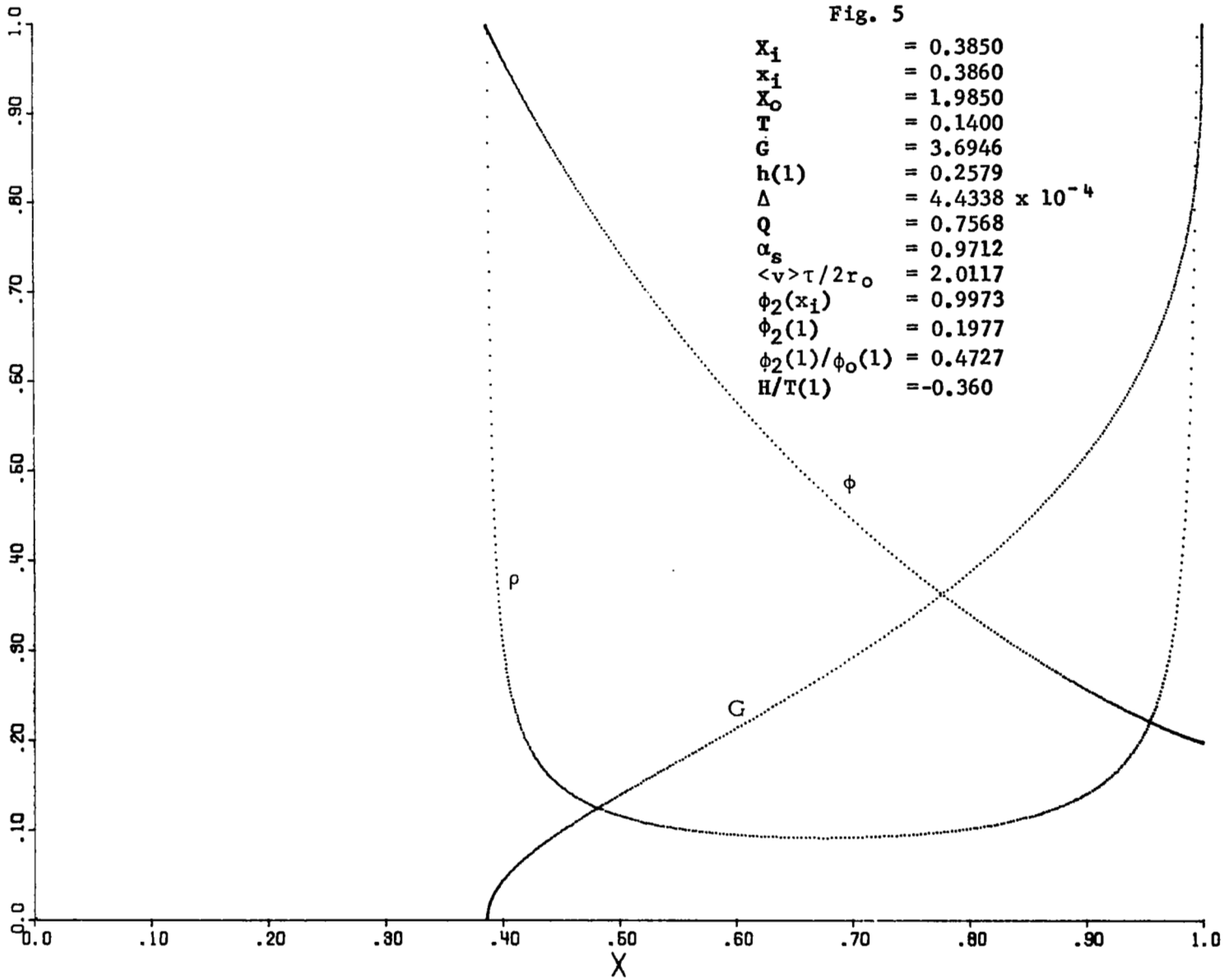
Fig. 5
X_i = 0.3850
x_i = 0.3860
X_o = 1.9850
T = 0.1400
G = 3.6946
h(1) = 0.2579
Δ = 4.4338 x 10^{-4}
Q = 0.7568
α_s = 0.9712
$\langle v \rangle \tau / 2r_o$ = 2.0117
$\phi_2(x_i)$ = 0.9973
$\phi_2(1)$ = 0.1977
$\phi_2(1)/\phi_o(1)$ = 0.4727
H/T(1) =-0.360
ϕ
ρ
G
0.0
.10
.20
.30
.40
.50
.60
.70
.80
.90
1.0
X

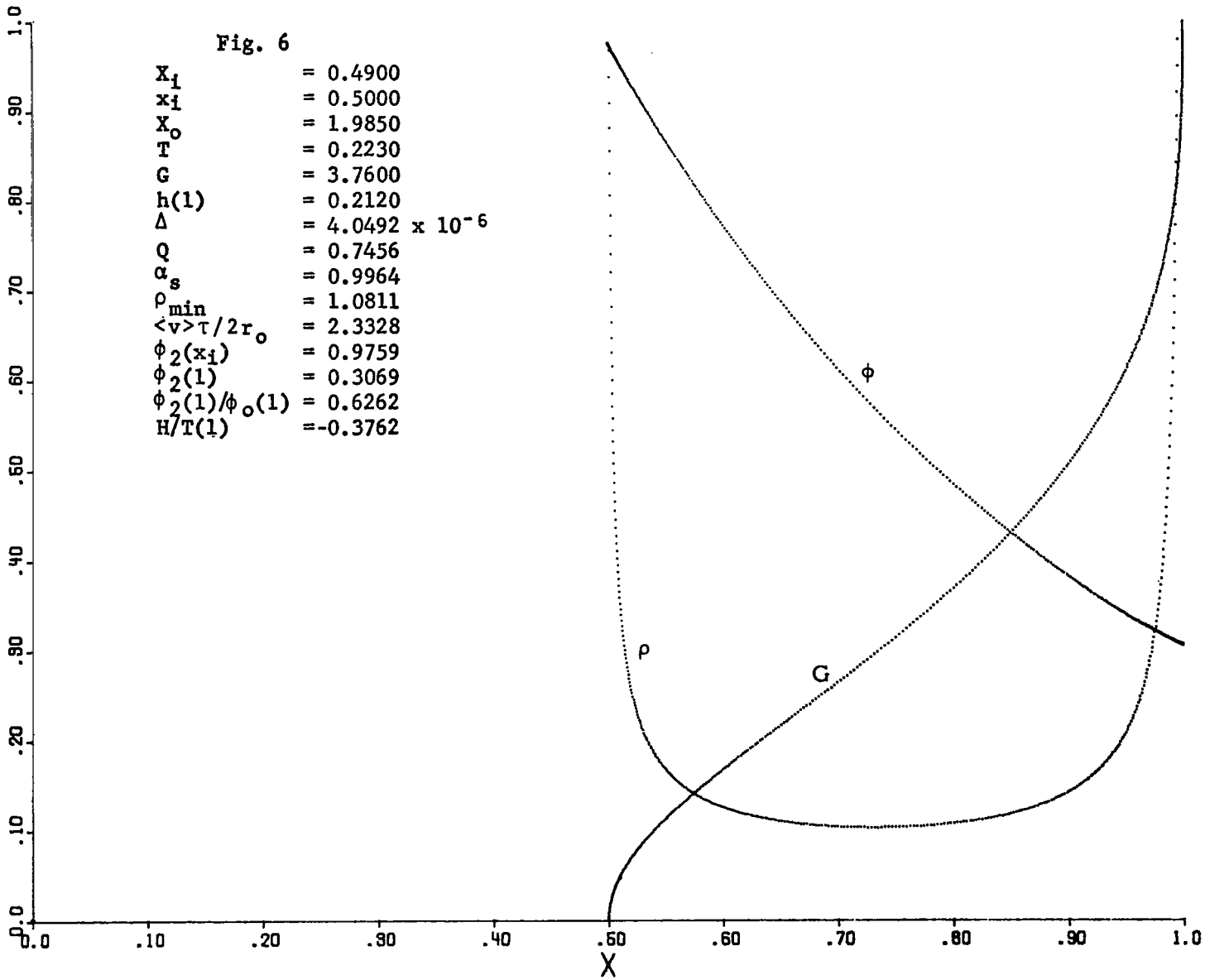
Fig. 6
X_i = 0.4900
x_i = 0.5000
X_o = 1.9850
T = 0.2230
G = 3.7600
h(1) = 0.2120
Δ = 4.0492 x 10^{-6}
Q = 0.7456
α_s = 0.9964
ρ_{min} = 1.0811
$\langle v \rangle \tau / 2r_o$ = 2.3328
$\phi_2(x_i)$ = 0.9759
$\phi_2(1)$ = 0.3069
$\phi_2(1)/\phi_o(1)$ = 0.6262
H/T(1) =-0.3762
ϕ
ρ
G
0.0
.10
.20
.30
.40
.50
.60
.70
.80
.90
1.0
X

Fig. 7

X_i	= 0.5900
x_i	= 0.6000
X_o	= 1.9850
T	= 0.3100
G	= 3.8199
h(1)	= 0.1721
Δ	= 3.6018×10^{-6}
Q	= 0.6880
α_s	= 0.9958
ρ_{min}	= 1.1602
$\langle v \rangle \tau / 2r_o$	= 2.6098
$\phi_2(x_i)$	= 0.9780
$\phi_2(1)$	= 0.4269
$\phi_2(1)/\phi_o(1)$	= 0.75536
H/T(1)	=-0.3770

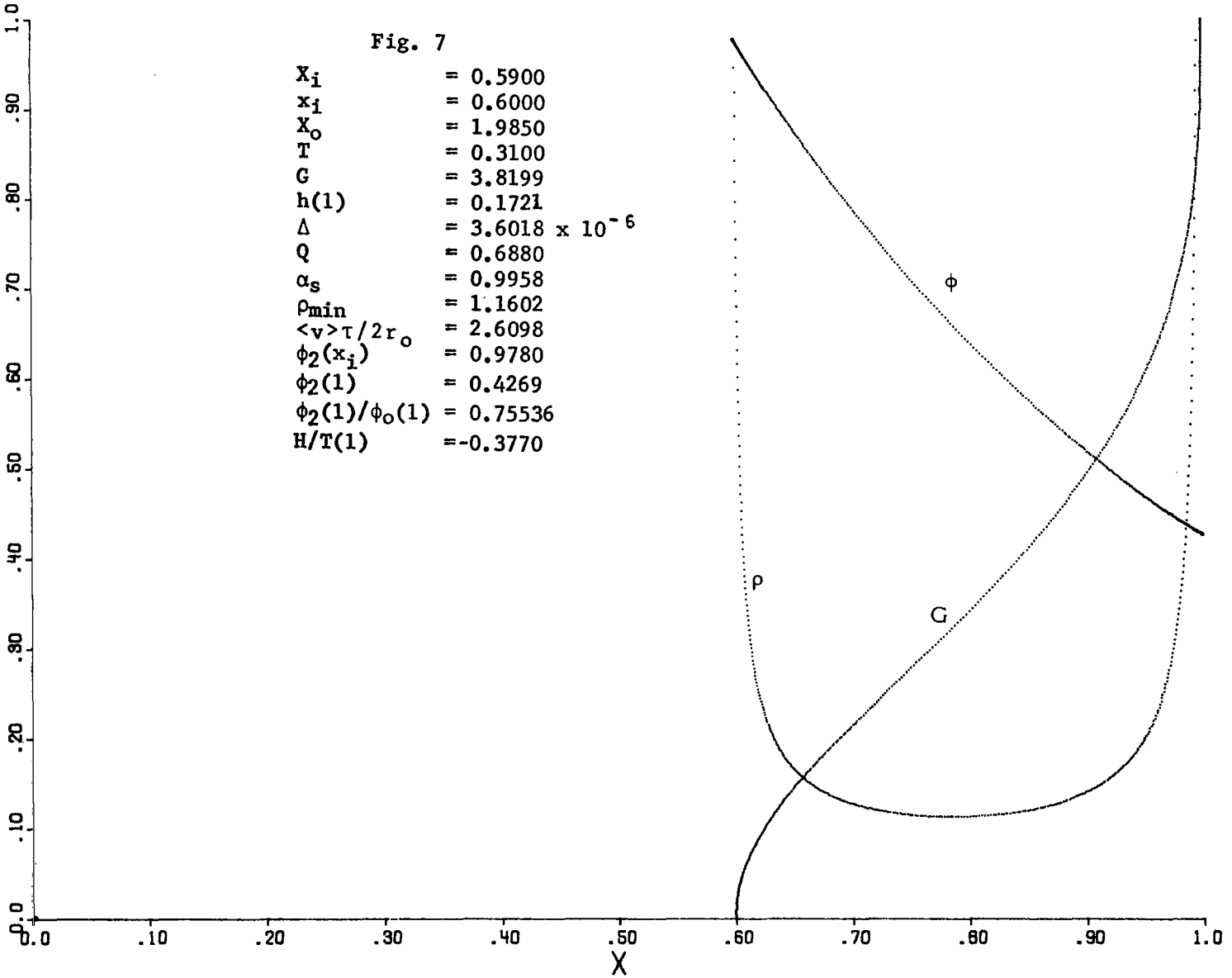

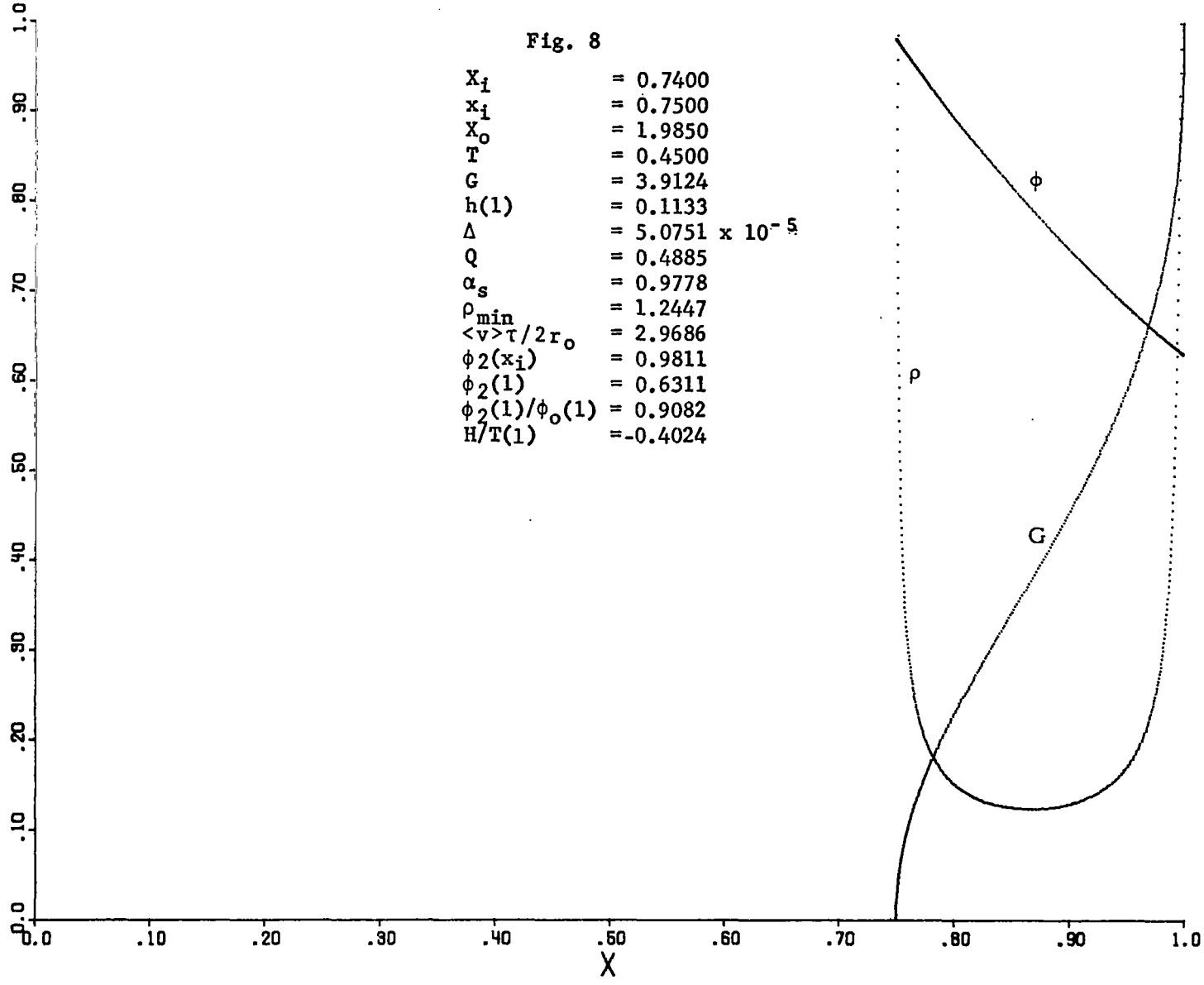
Fig. 8
X_i = 0.7400
x_i = 0.7500
X_o = 1.9850
T = 0.4500
G = 3.9124
h(1) = 0.1133
Δ = 5.0751 x 10^{-5}
Q = 0.4885
α_s = 0.9778
ρ_{min} = 1.2447
$\langle v \rangle \tau / 2r_o$ = 2.9686
$\phi_2(x_i)$ = 0.9811
$\phi_2(1)$ = 0.6311
$\phi_2(1)/\phi_o(1)$ = 0.9082
H/T(1) = -0.4024
ϕ
ρ
G
0.0
.10
.20
.30
.40
.50
.60
.70
.80
.90
1.0
X

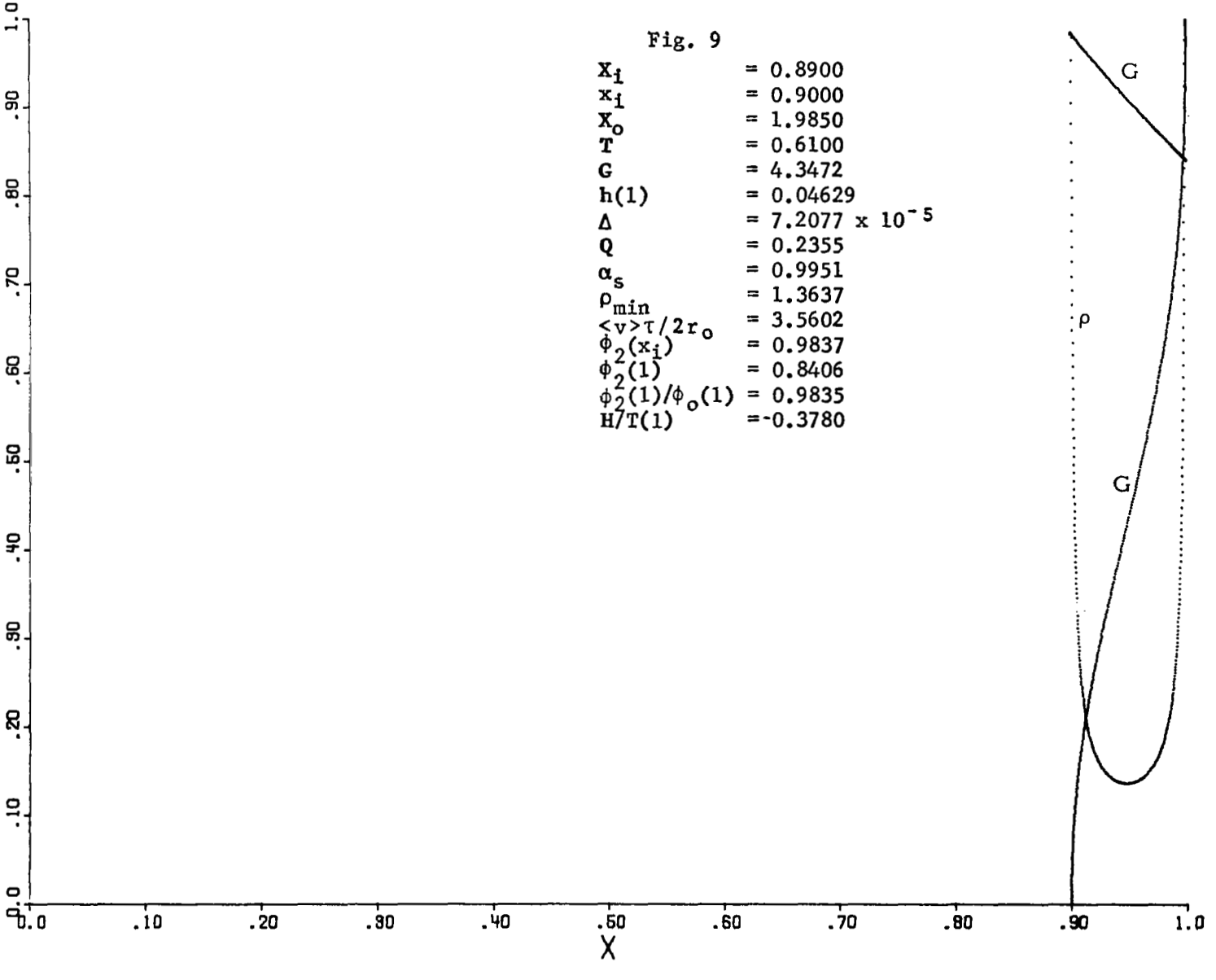

Fig. 9

X_i	= 0.8900
x_i	= 0.9000
X_o	= 1.9850
T	= 0.6100
G	= 4.3472
h(1)	= 0.04629
Δ	= 7.2077×10^{-5}
Q	= 0.2355
α_s	= 0.9951
ρ_{min}	= 1.3637
$\langle v \rangle \tau / 2r_o$	= 3.5602
$\phi_2(x_i)$	= 0.9837
$\phi_2(1)$	= 0.8406
$\phi_2(1)/\phi_o(1)$	= 0.9835
H/T(1)	=-0.3780

Fig. 10

$H \approx -0.4$

Summary of data from Fig.s 3 thru 9

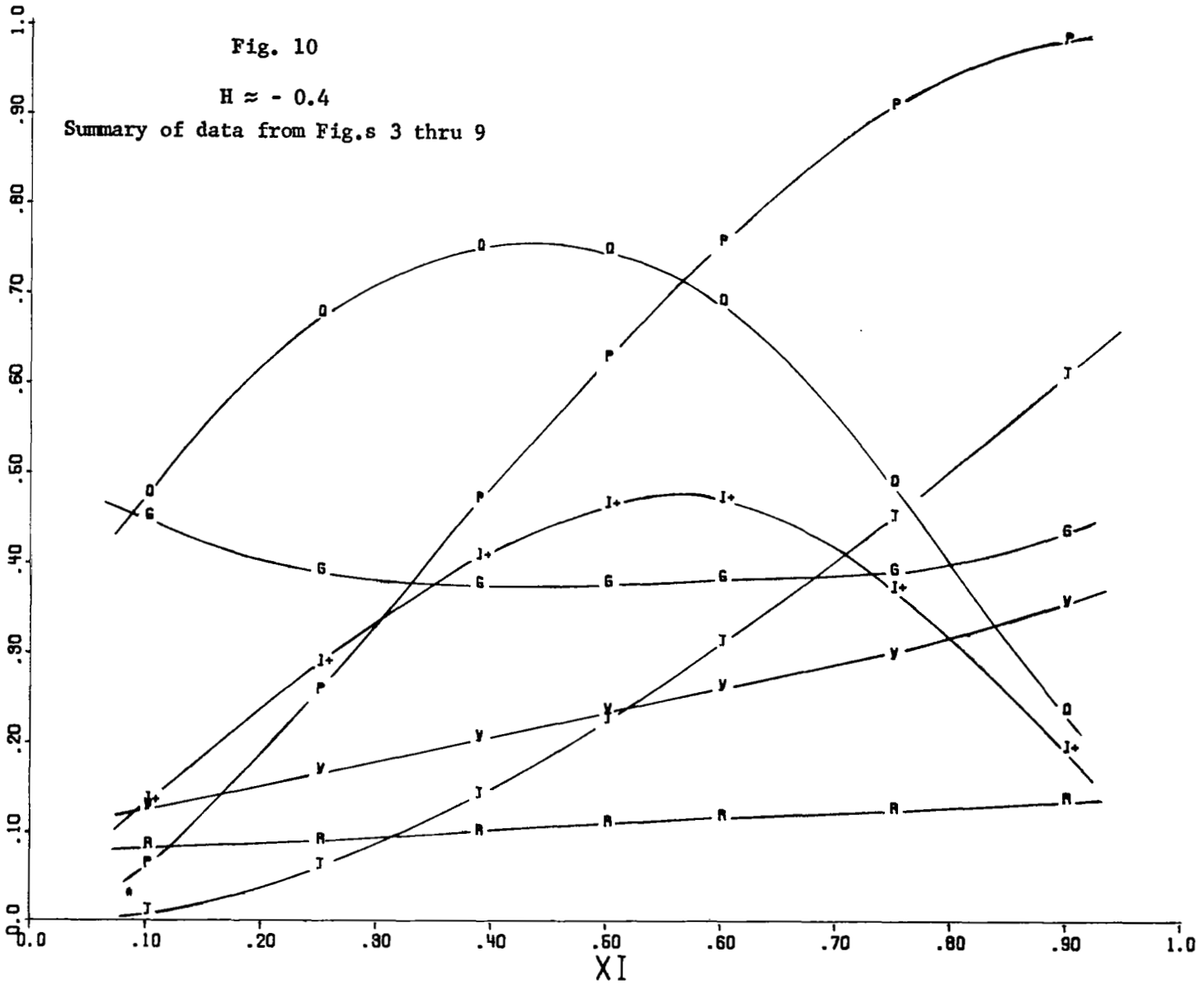

Fig. 11

X_i	= 0.0980
x_i	= 0.1000
X_o	= 1.6500
T	= 9.895×10^{-3}
G	= 4.4618
h(1)	= 0.3427
Δ	= 9.8510×10^{-4}
Q	= 0.4755
α_s	= 0.9557
ρ_{min}	= 0.8158
$\langle v \rangle \tau / 2r_o$	= 1.2475
$\phi_2(x_i)$	= 0.9900
$\phi_2(1)$	= 0.0104
$\phi_2(1)/\phi_o(1)$	= 0.0585
H/T(1)	=-.0480

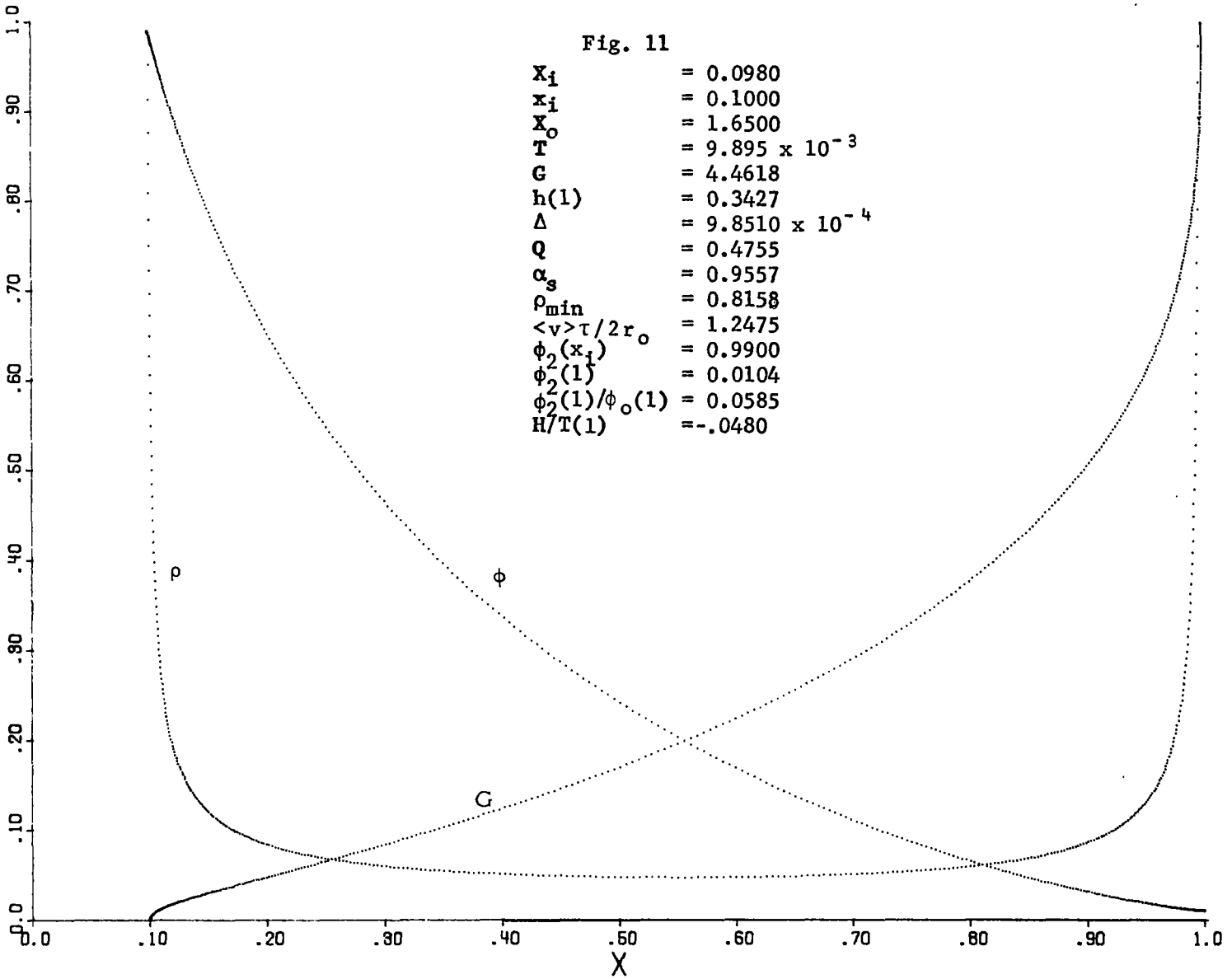

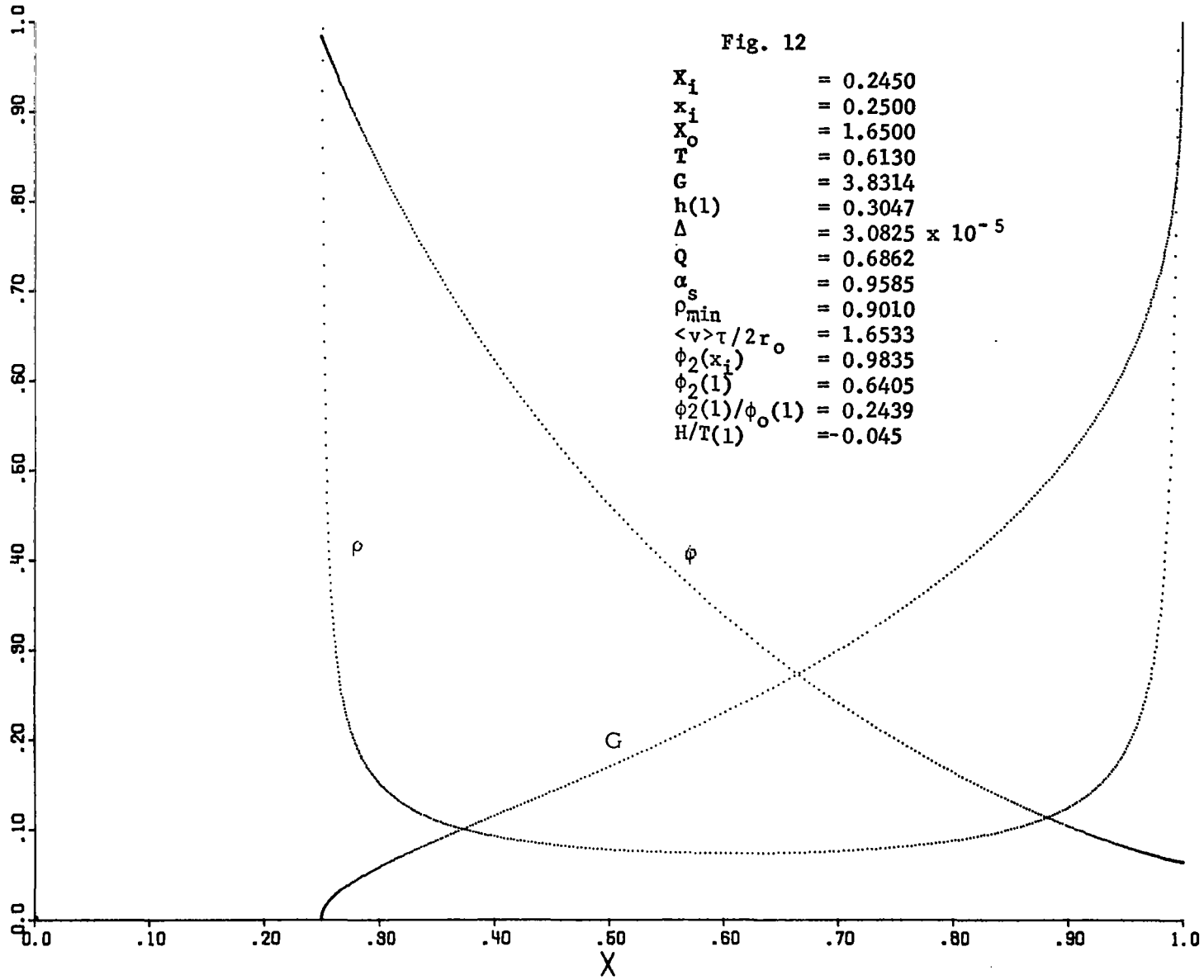
Fig. 12
X_i = 0.2450
x_i = 0.2500
X_o = 1.6500
T = 0.6130
G = 3.8314
h(1) = 0.3047
Δ = 3.0825 x 10^{-5}
Q = 0.6862
α_s = 0.9585
ρ_{min} = 0.9010
$\langle v \rangle \tau / 2r_o$ = 1.6533
$\phi_2(x_i)$ = 0.9835
$\phi_2(1)$ = 0.6405
$\phi_2(1)/\phi_o(1)$ = 0.2439
H/T(1) =-0.045
ρ
φ
G
0.0
.10
.20
.30
.40
.50
.60
.70
.80
.90
1.0
X

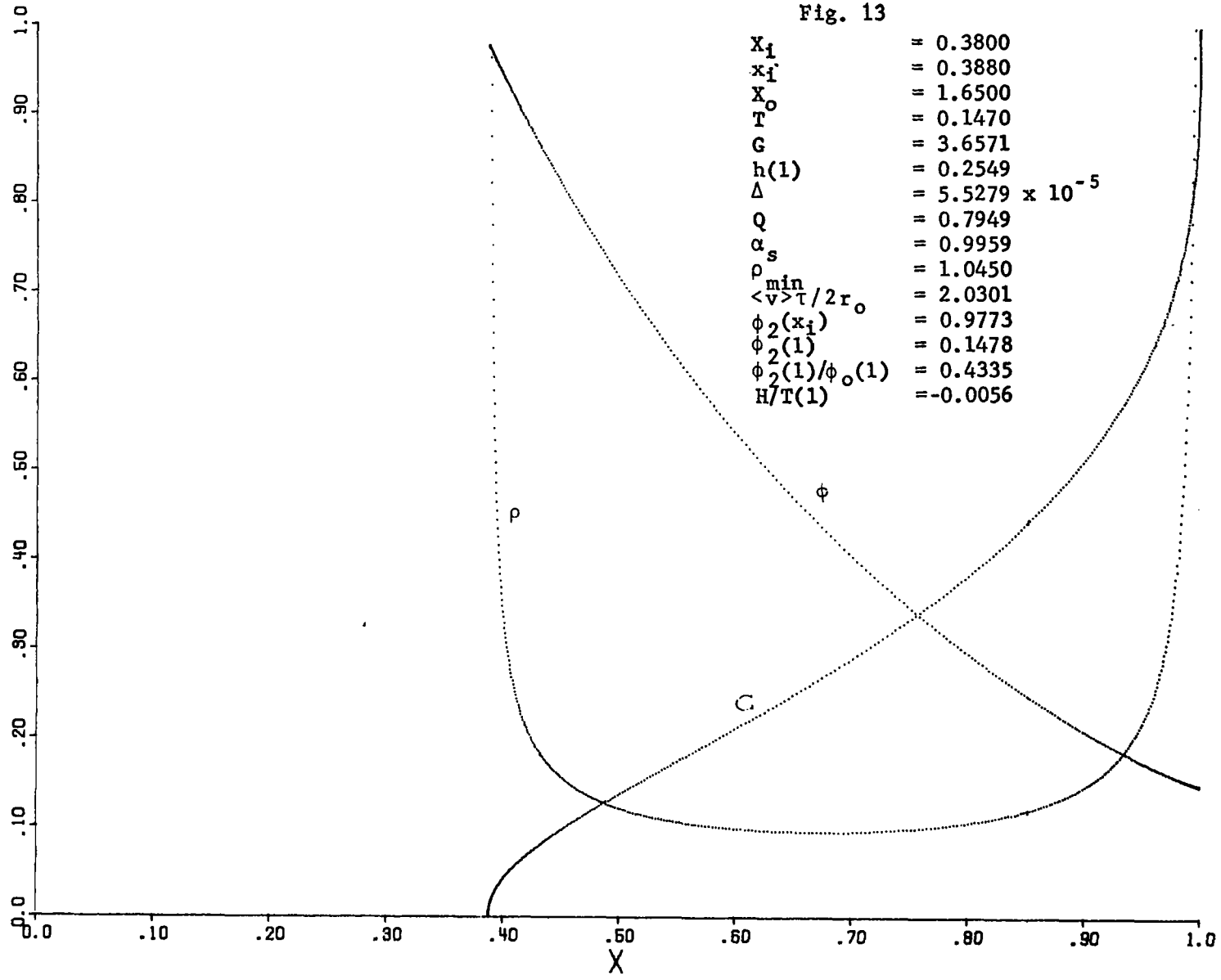
Fig. 13
X_i = 0.3800
x_i = 0.3880
X_o = 1.6500
T = 0.1470
G = 3.6571
h(1) = 0.2549
Δ = 5.5279 x 10^{-5}
Q = 0.7949
α_s = 0.9959
ρ_{min} = 1.0450
$\langle v \rangle \tau / 2r_o$ = 2.0301
$\phi_2(x_i)$ = 0.9773
$\phi_2(1)$ = 0.1478
$\phi_2(1)/\phi_o(1)$ = 0.4335
H/T(1) =-0.0056
ρ
φ
C
0.0
.10
.20
.30
.40
.50
.60
.70
.80
.90
1.0
X

Fig. 14

X_i	= 0.4900
x_i	= 0.5000
X_o	= 1.6500
T	= 0.2430
G	= 3.5944
h(1)	= 0.2123
Δ	$=-4.3523 \times 10^{-4}$
Q	= 0.8117
α_s	= 0.9945
ρ_{min}	= 1.1773
$\langle v \rangle \tau / 2r_o$	= 2.3310
$\phi_2(x_i)$	= 0.9737
$\phi_2'(1)$	= 0.2447
$\phi_2(1)/\phi_o(1)$	= 0.5933
H/T(1)	=-0.0071

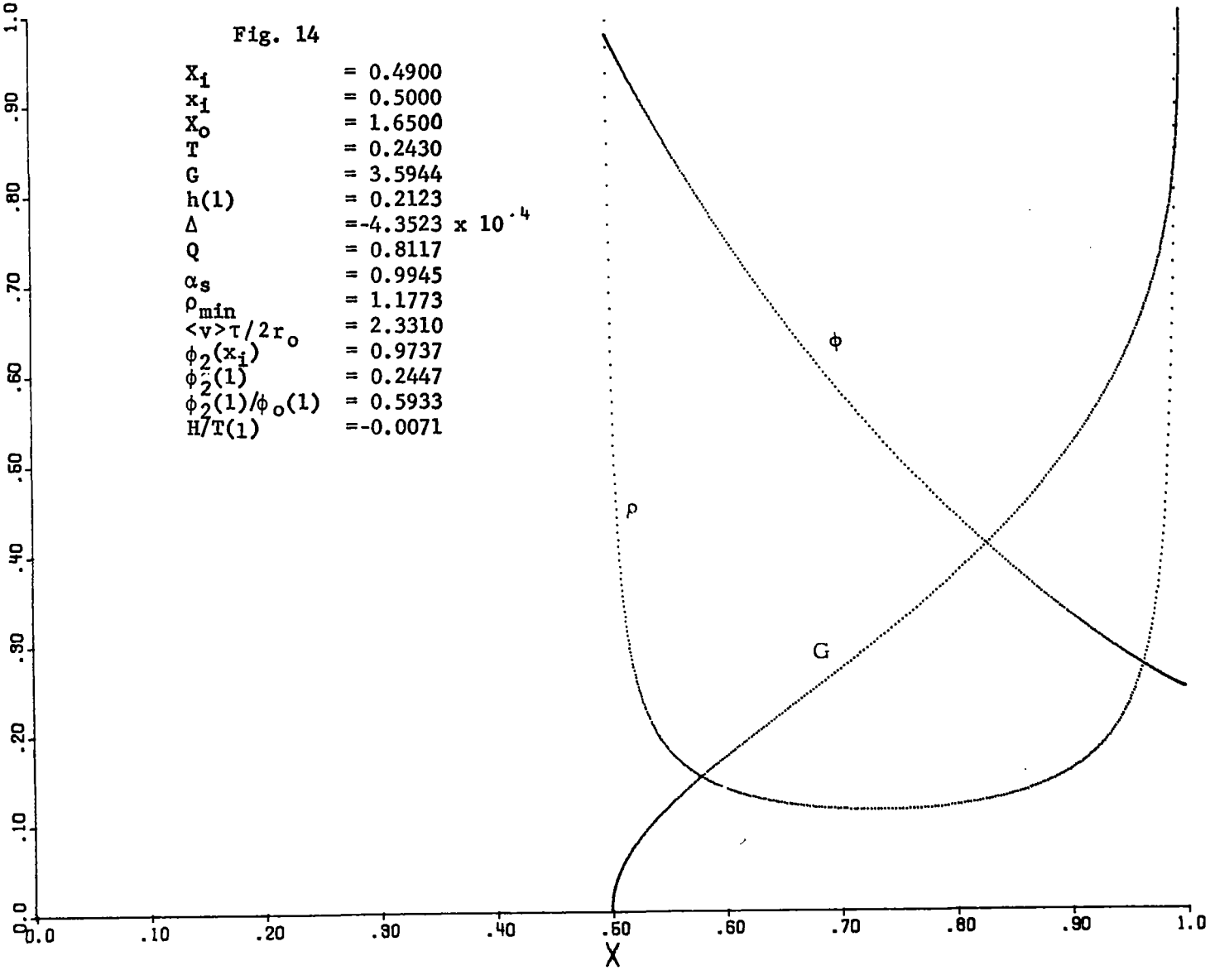

Fig. 15

X_i	= 0.5900
x_i	= 0.6000
X_o	= 1.6500
T	= 0.3500
G	= 3.5867
h(1)	= 0.1724
Δ	= 3.0415×10^{-6}
Q	= 0.7749
α_s	= 0.9933
ρ_{min}	= 1.3098
$\langle v \rangle \tau / 2r_o$	= 2.6048
$\phi_2(x_i)$	= 0.9751
$\phi_2(1)$	= 0.3529
$\phi_2(1)/\phi_o(1)$	= 0.7247
$H'T(1)$	=-0.0083

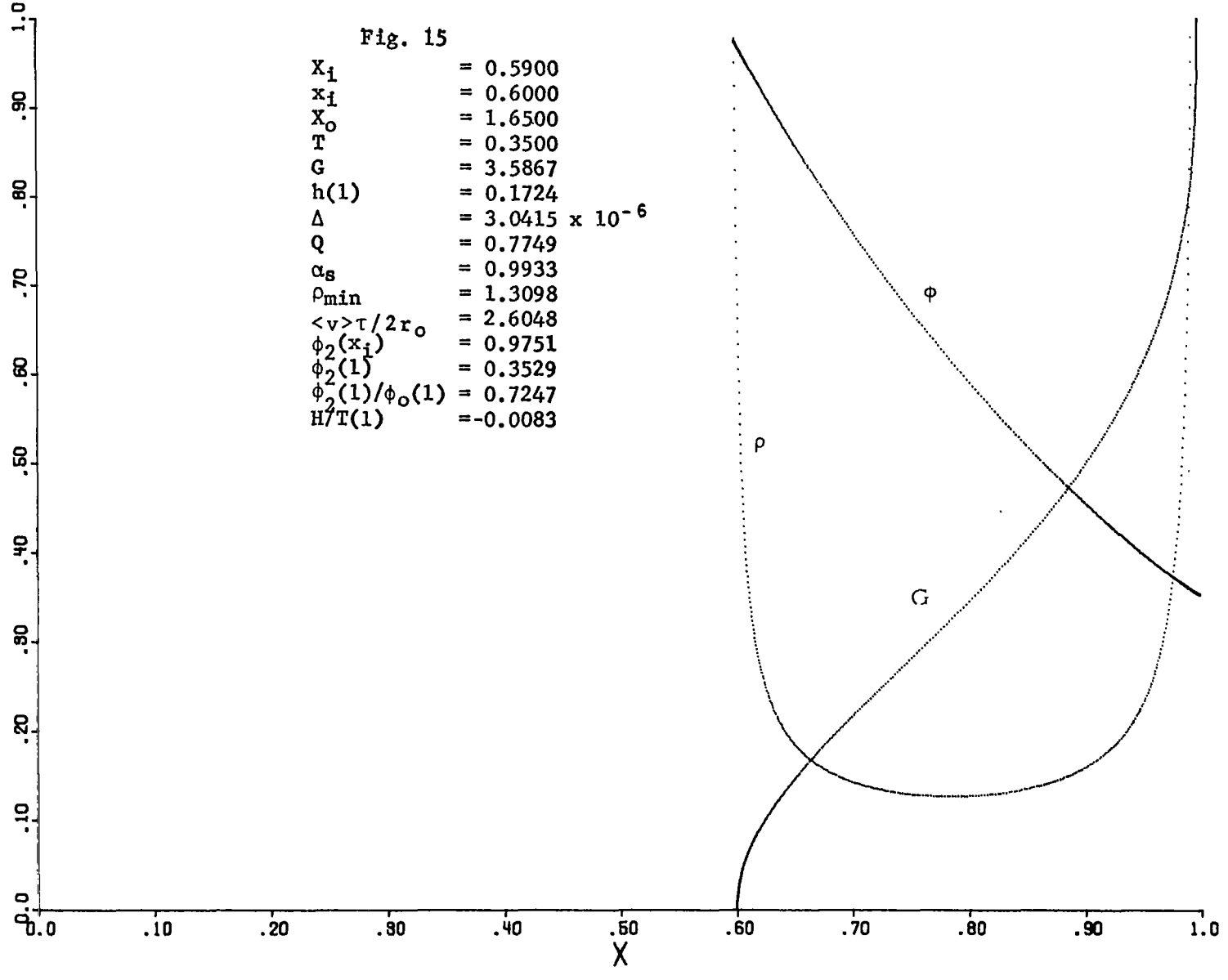

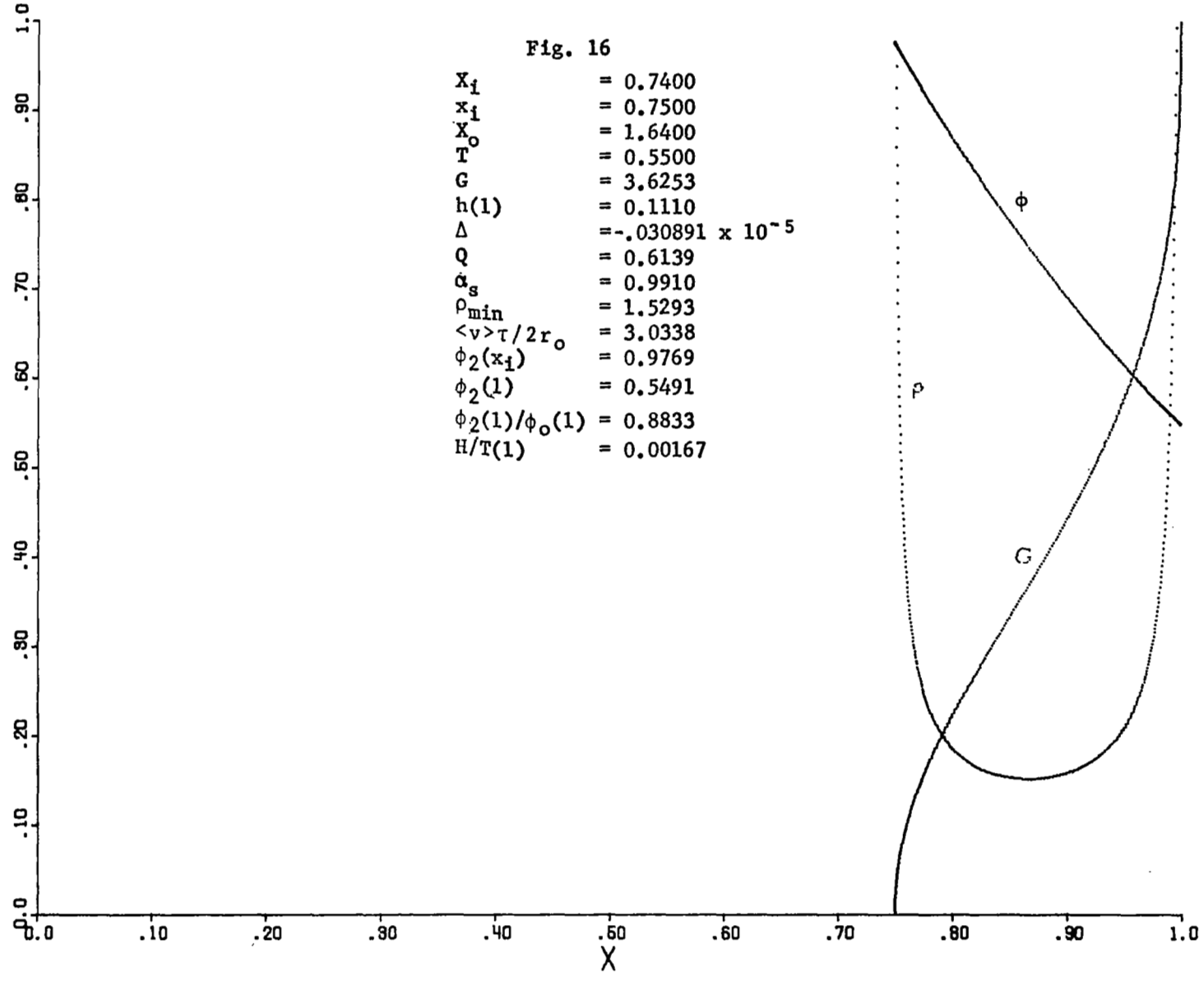
Fig. 16
X_i = 0.7400
x_i = 0.7500
X_o = 1.6400
T = 0.5500
G = 3.6253
h(1) = 0.1110
Δ =-.030891 x 10^{-5}
Q = 0.6139
α_s = 0.9910
ρ_{min} = 1.5293
$\langle v \rangle \tau / 2r_o$ = 3.0338
$\phi_2(x_i)$ = 0.9769
$\phi_2(1)$ = 0.5491
$\phi_2(1)/\phi_o(1)$ = 0.8833
H/T(1) = 0.00167
ϕ
ρ
G
0.0
.10
.20
.30
.40
.50
.60
.70
.80
.90
1.0
X

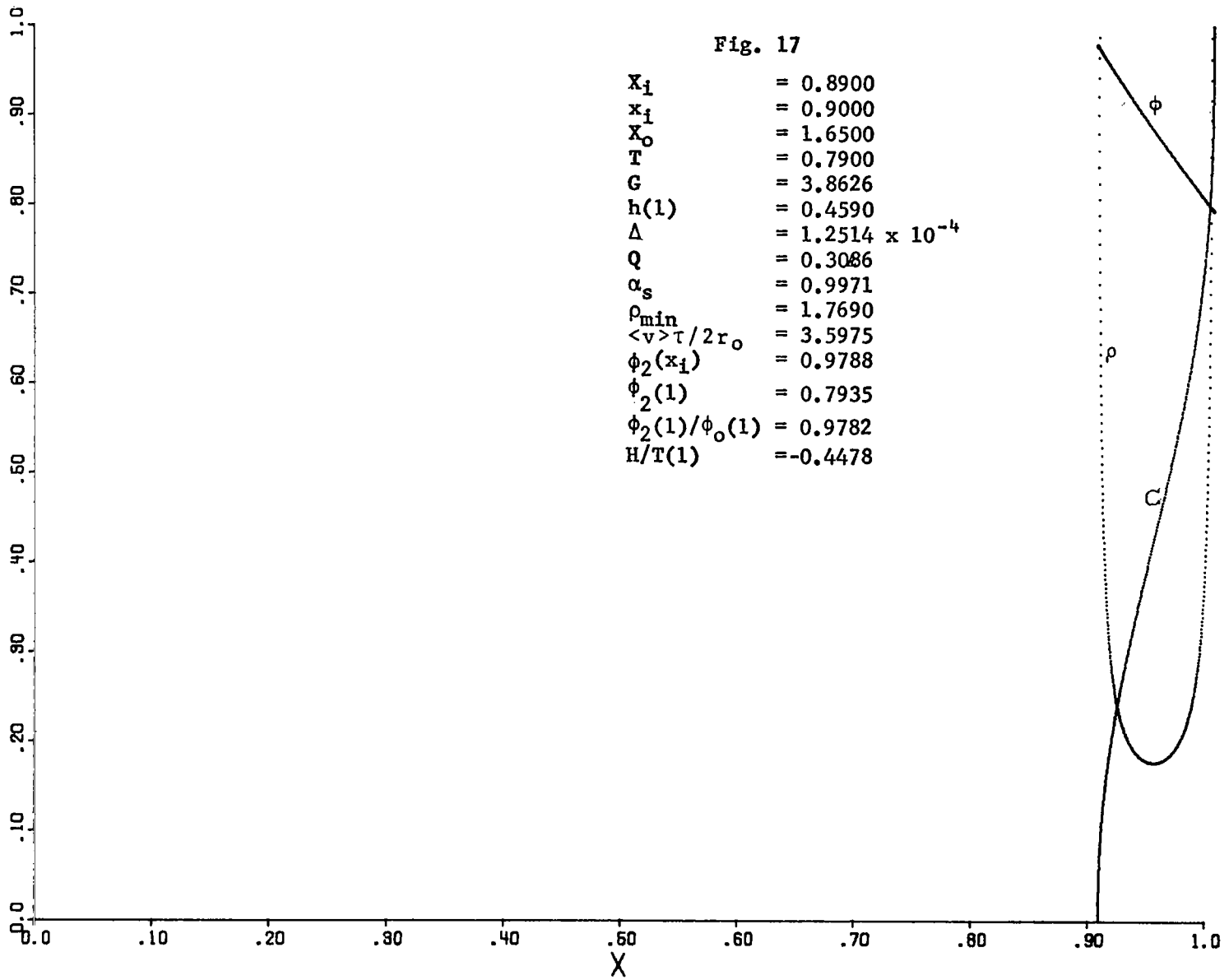

Fig. 17

X_i	= 0.8900
x_i	= 0.9000
X_o	= 1.6500
T	= 0.7900
G	= 3.8626
h(1)	= 0.4590
Δ	= 1.2514×10^{-4}
Q	= 0.3086
α_s	= 0.9971
ρ_{min}	= 1.7690
$\langle v \rangle \tau / 2 r_o$	= 3.5975
$\phi_2(x_i)$	= 0.9788
$\phi_2(1)$	= 0.7935
$\phi_2(1)/\phi_o(1)$	= 0.9782
H/T(1)	=-0.4478

Fig. 18

H ≈ 0.0

Summary of data from Figs. 11 thru 17

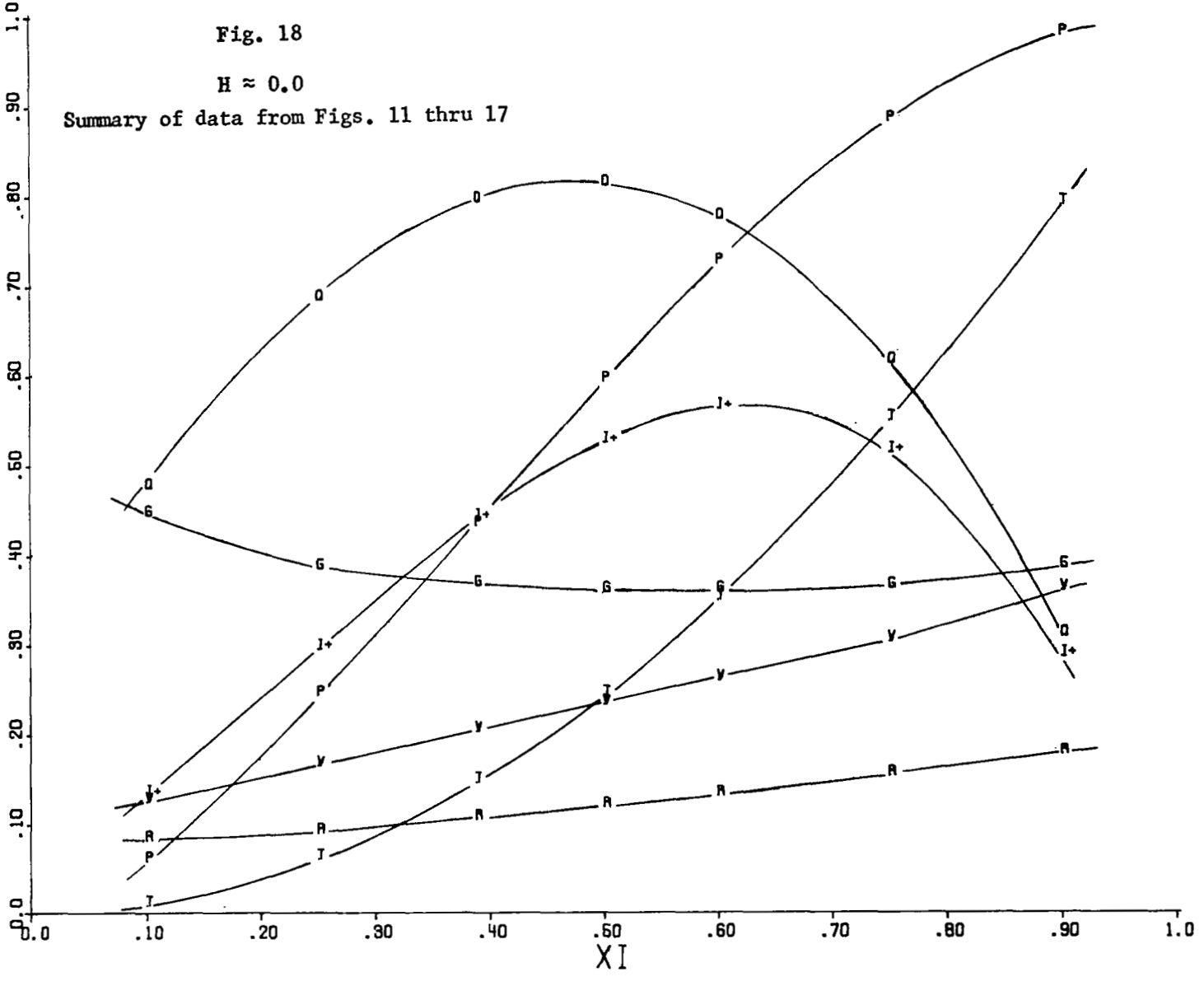

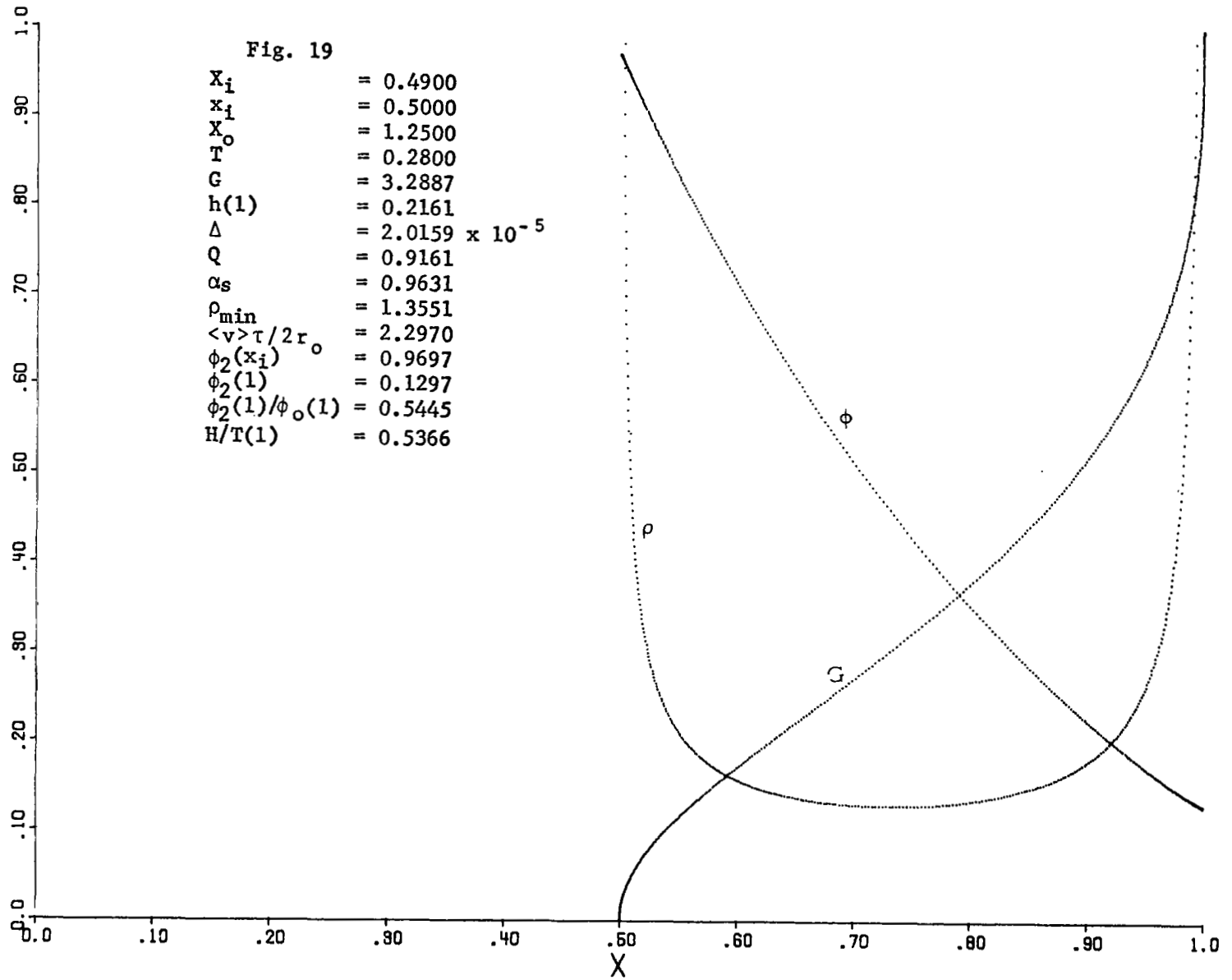
Fig. 19
X_i = 0.4900
x_i = 0.5000
X_o = 1.2500
T = 0.2800
G = 3.2887
h(1) = 0.2161
Δ = 2.0159 x 10^{-5}
Q = 0.9161
α_s = 0.9631
ρ_{min} = 1.3551
$\langle v \rangle \tau / 2r_o$ = 2.2970
$\phi_2(x_i)$ = 0.9697
$\phi_2(1)$ = 0.1297
$\phi_2(1)/\phi_o(1)$ = 0.5445
H/T(1) = 0.5366
ϕ
ρ
G
0.0
.10
.20
.30
.40
.50
.60
.70
.80
.90
1.0
X

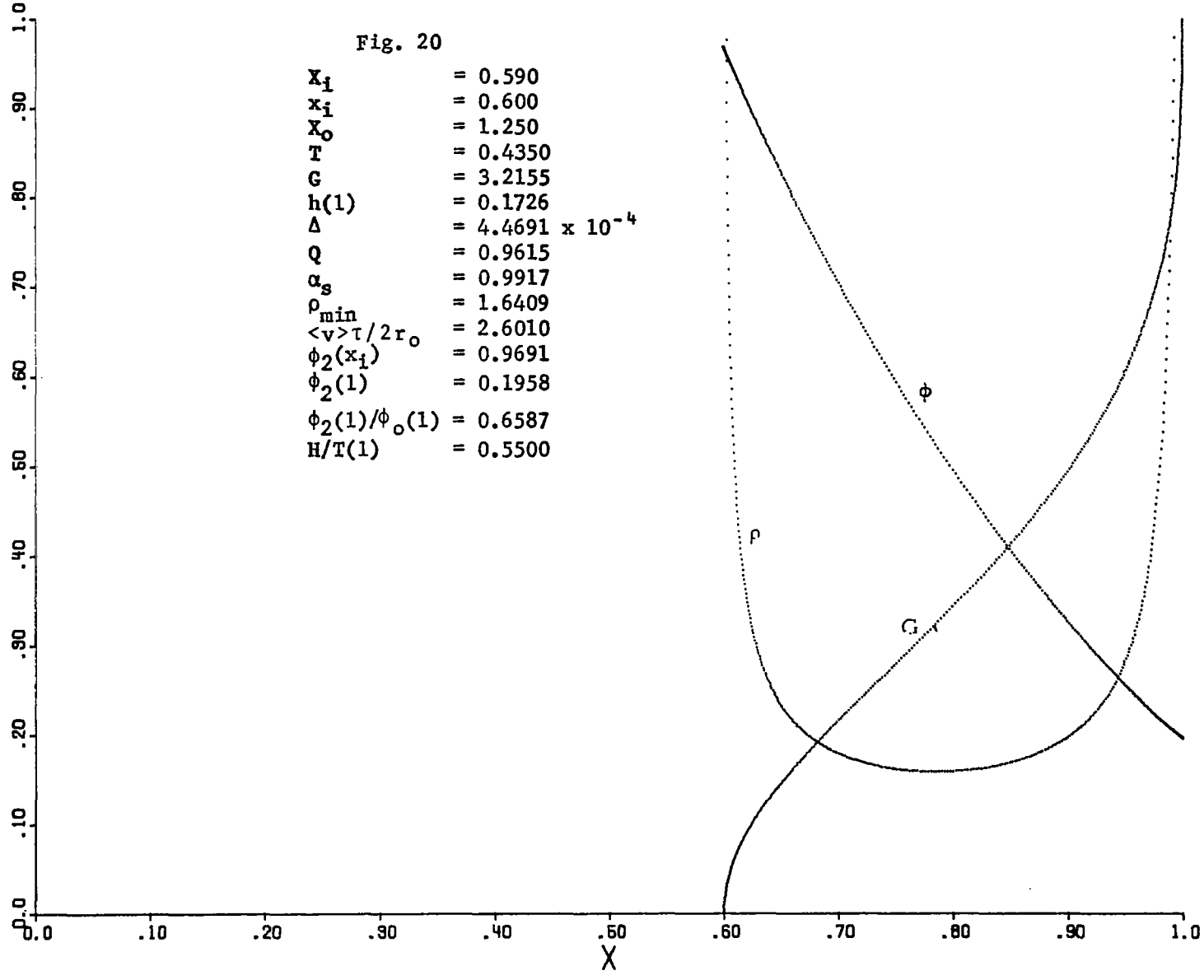
Fig. 20
X_i = 0.590
x_i = 0.600
X_o = 1.250
T = 0.4350
G = 3.2155
h(1) = 0.1726
Δ = 4.4691 x 10^{-4}
Q = 0.9615
α_s = 0.9917
ρ_{min} = 1.6409
$\langle v \rangle \tau / 2r_o$ = 2.6010
$\phi_2(x_i)$ = 0.9691
$\phi_2(1)$ = 0.1958
$\phi_2(1)/\phi_o(1)$ = 0.6587
H/T(1) = 0.5500
ϕ
ρ
G
0.0
.10
.20
.30
.40
.50
.60
.70
.80
.90
1.0
X

Fig. 21

X_i	= 0.740
x_i	= 0.750
X_o	= 1.250
T	= .7850
G	= 2.9895
h(1)	= 0.1124
Δ	= 8.8623×10^{-5}
Q	= 0.8617
α_s	= 0.98288
ρ_{min}	= 2.17742
$\langle v \rangle \tau / 2r_o$	= 2.99388
$\phi_2(x_i)$	= 0.96699
$\phi_2(1)$	= 0.35644
$\phi_2(1)/\phi_o(1)$	= 0.8374
H/T(1)	= 0.54594

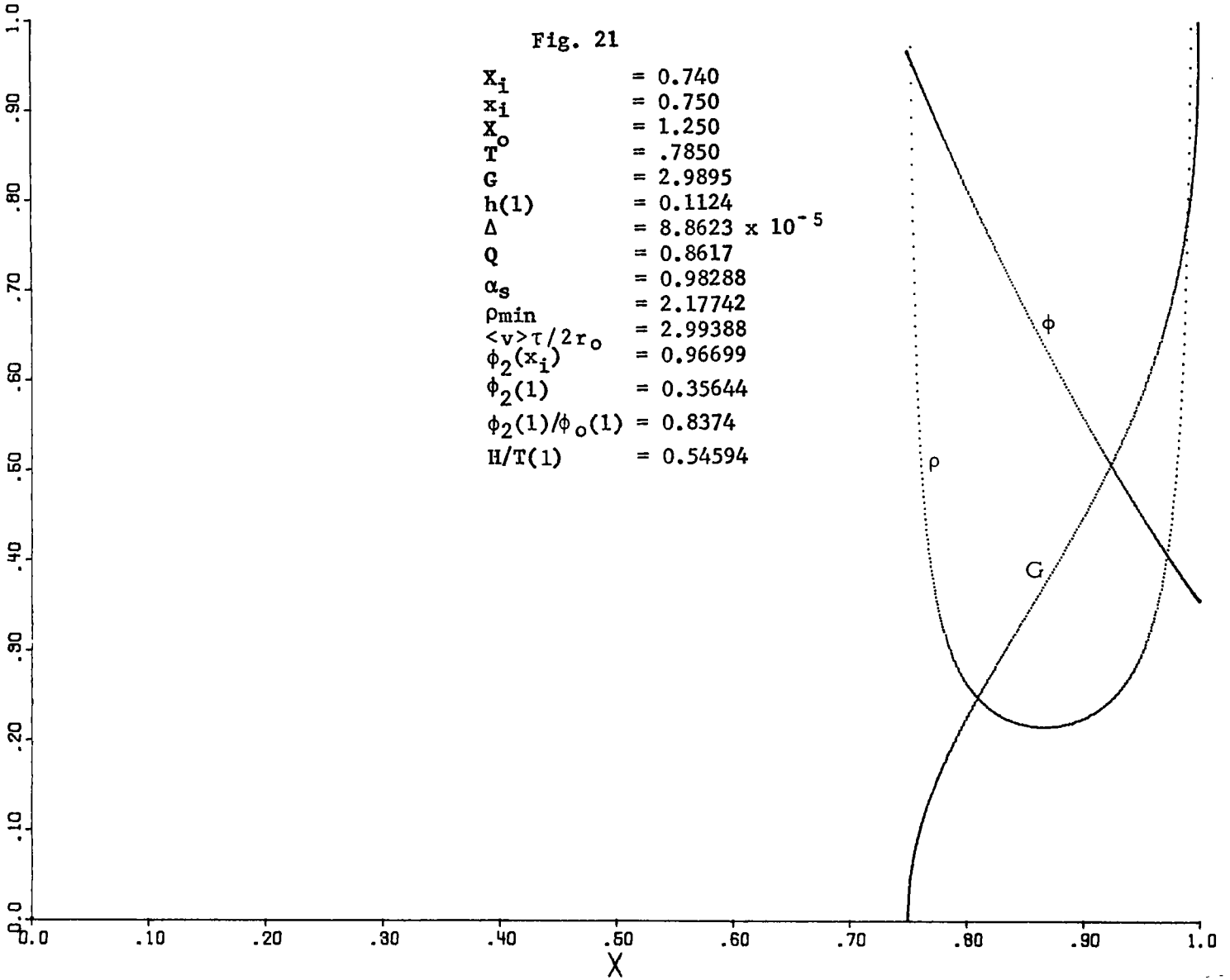

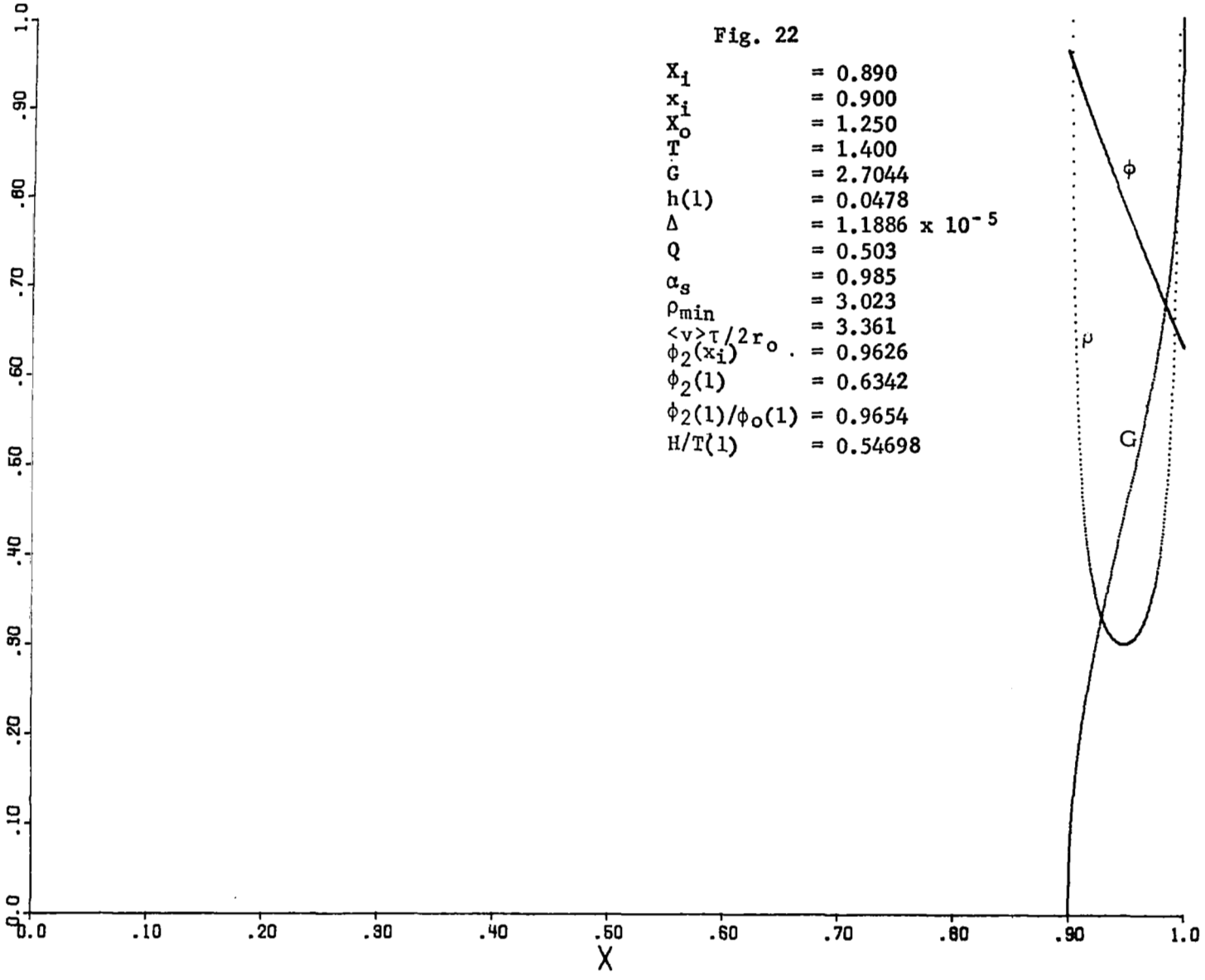

Fig. 22

X_i	= 0.890
x_i	= 0.900
X_o	= 1.250
T	= 1.400
G	= 2.7044
h(1)	= 0.0478
Δ	= 1.1886×10^{-5}
Q	= 0.503
α_s	= 0.985
ρ_{min}	= 3.023
$\langle v \rangle \tau / 2 r_o$	= 3.361
$\phi_2(x_i)$	= 0.9626
$\phi_2(1)$	= 0.6342
$\phi_2(1)/\phi_o(1)$	= 0.9654
H/T(1)	= 0.54698

Fig. 23

H ≈ 0.55

Summary of data from Figs. 19 thru 22

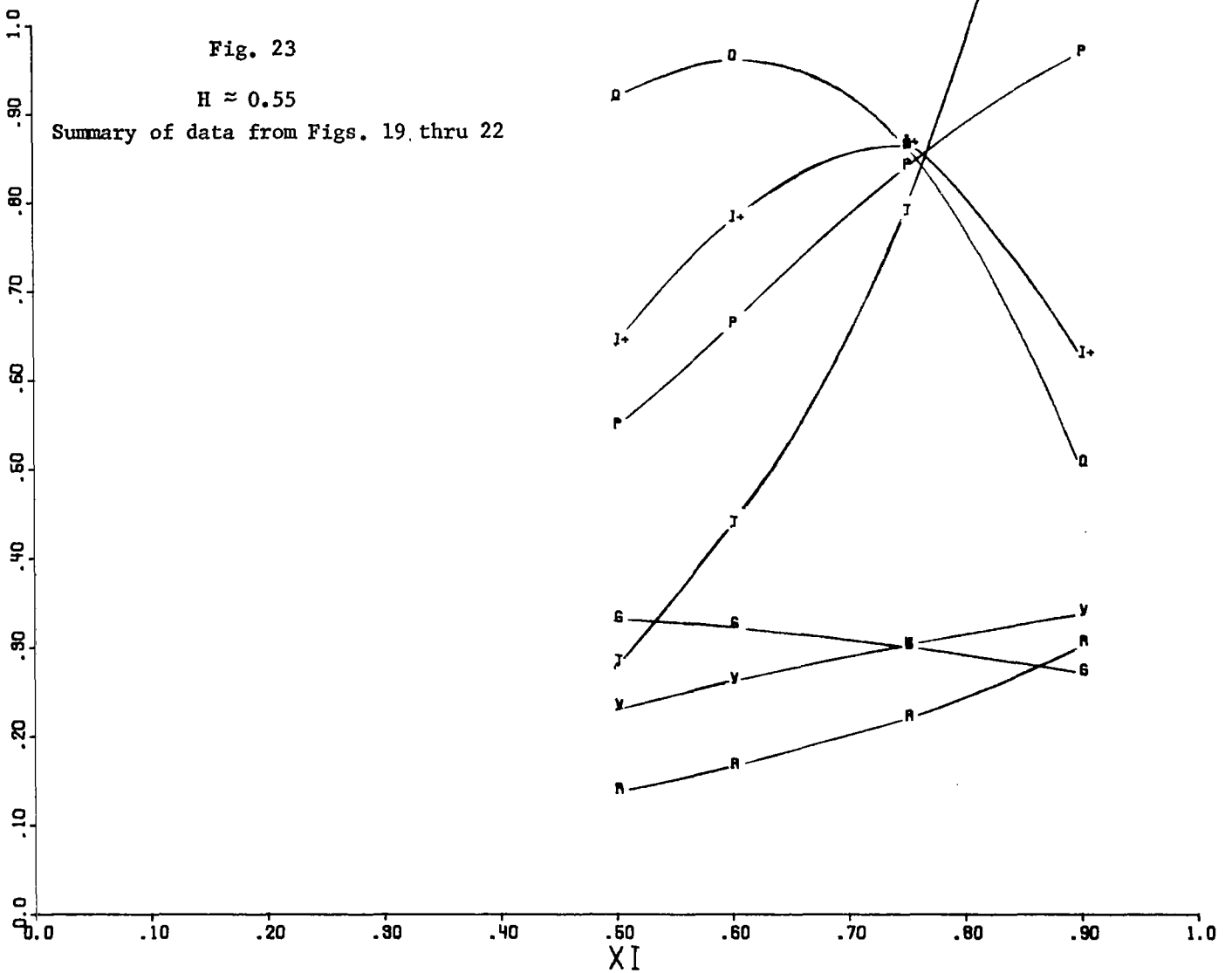

Application

Below, a particular orbitron solution is applied to a particular orbitron configuration. The machine solution selected is neither a maximum or minimum solution but only typical. From the data of Fig. 18

$$X_i = 0.490 \quad \text{(Machine Record)}$$

$$x_i = 0.500 \quad \text{(Machine Record)}$$

$$\frac{T(1)}{eV} = 0.243 \quad \text{(T Curve)}$$

$$\frac{eN_L}{2\pi\epsilon V} = 0.811 \quad \text{(Q Curve)}$$

$$\frac{\mathring{N}_L^+}{n_g \sigma(\langle v \rangle) \left[\frac{2\pi\epsilon V}{e}\right] \left(\frac{2eV}{m}\right)^{\frac{1}{2}}} = 0.526 \left(\frac{\tau}{2r} \langle v \rangle \frac{Q}{G}, \text{ I+ Curve}\right)$$

$$\frac{\tau}{2r_o} \langle v \rangle = 2.33 \quad \text{(V Curve)}$$

$$\left(\frac{2eV}{m}\right)^{\frac{1}{2}} \frac{\tau}{2r_o} = 3.59 \quad \text{(G Curve)}$$

$$\alpha_s = 0.994 \quad \text{(from machine record)}$$

$$X_o = 1.65 \quad \text{(from H=0)}$$

Prescribe:

Outer turning point kinetic energy $\equiv T(1) = 100\text{eV}$

Outer cylinder radius $\equiv R_o = 2.5 \times 10^{-2}$ m

Then from these data it follows:

$$\text{Outer turning point radius} \equiv r_o = \frac{2.5 \times 10^{-2}}{1.65}$$

$$= 1.52 \times 10^{-2} \text{ m}$$

$$\text{Anode radius} \equiv R_i = (0.49)(1.52 \times 10^{-2})$$

$$= 0.743 \times 10^{-2} \text{ m}$$

$$\text{Anode voltage} \equiv V = \frac{100}{0.243} = 412 \text{ Volts}$$

$$\frac{\text{Number of electrons}}{\text{unit length}} \equiv N_L = \frac{2\pi(8.85 \times 10^{-12})(0.811)}{1.6 \times 10^{-19}}$$

$$= 1.16 \times 10^{11} \text{ m}^{-1}$$

$$(= 1.16 \times 10^{9} \text{ cm}^{-1})$$

$$\text{Minimum Charge Density} \equiv \rho_{min} = -\frac{1.18(8.85 \times 10^{-12})(412)}{(1.52 \times 10^{-2})^2}$$

$$= -1.86 \times 10^{-5}\ C/m^3$$

$$(= -1.86 \times 10^{-11}\ C/cm^3)$$

$$\text{Minimum } \frac{\text{number of electrons}}{\text{unit volume}} \equiv \frac{\rho_{min}}{-e} = \frac{-1.86 \times 10^{-11}}{-1.6 \times 10^{-19}}$$

$$= 1.16 \times 10^{8}\ cm^{-3}$$

$$\text{Orbit Period} \equiv \tau = (3.59)(3.03 \times 10^{-2})\left[\frac{9.1 \times 10^{-31}}{3.2 \times 10^{-19}(412)}\right]^{\frac{1}{2}}$$

$$= 9.0 \times 10^{-9}\ sec$$

$$\text{Average Kinetic Energy} \equiv \langle T \rangle = \frac{m}{2}\langle v \rangle^2$$

$$= \frac{9.1 \times 10^{-31}}{2}\left[\frac{(2.33)(3.03 \times 10^{-2})}{9 \times 10^{-9}}\right]^2$$

$$= 2.82 \times 10^{-17} J$$

$$(= 175.5 eV)$$

$$\text{Argon Cross Section} \equiv \sigma_{A_r^+}\ (\langle T \rangle = 175.5 eV) \approx 2.9 \times 10^{-20}\ m^2$$

$$\frac{\text{Ion Current}}{\text{unit length} \cdot n_g} \equiv \frac{e\mathring{N}_L^+}{n_g} = (0.526)\ \sigma_{A_r^+}\ (2\pi\epsilon V)\left[\frac{2eV}{m}\right]^{\frac{1}{2}}$$

$$= 4.2 \times 10^{-21}\ \frac{A}{m}\ \frac{l}{n_g}$$

$$\frac{\text{Ion Current}}{\text{unit length}\cdot\text{Torr}} \equiv \frac{e\mathring{N}_L^+}{P_T} = \frac{e\mathring{N}_L^+}{n_g}\ (3.2 \times 10^{22})$$

$$= 137\ \frac{\text{Amp}}{\text{m Torr}}$$

$$\left(= 1.37\ \frac{\text{Amp}}{\text{cm Torr}}\right)$$

$$\frac{\text{Ionic Pumping Speed}}{\text{unit length}} \equiv S_L = \frac{\mathring{N}_L^+}{n_g} = 2.6 \times 10^{-2}\ \frac{m^3}{sec}\ \frac{1}{m}$$

$$\left(= 0.26\ \frac{\text{liters}}{\text{sec cm}}\right)$$

The above example is a rather low voltage device. Consider now the effect resulting from increasing the outer turning point kinetic energy by an order of magnitude. If it is prescribed that $T(r_o) = 10^3 eV$, and all other prescribed parameters remain as above, the geometrical parameters do not change and the derived parameters are as follows:

Anode oltage: $V = 4120$ volts

$\frac{\text{Number of electrons}}{\text{unit length}}$: $N_L = 1.16 \times 10^{10}\ cm^{-1}$

Orbit period: $\tau = 2.85 \times 10^{-9}$ sec

Average kinetic energy: $\langle T \rangle = 1755$ eV

Argon cross section (at $\langle T \rangle = 1755 eV$): $\sigma_{A_r^+} \approx .79 \times 10^{-16} cm^2$

$\frac{\text{Ion current}}{\text{unit length}\cdot\text{Torr}}$: $\frac{e\mathring{N}_L^+}{P_T} = 11.9\ \frac{\text{Amp}}{\text{cm Torr}}$

$\frac{\text{Ionic pumping speed}}{\text{unit length}}$: $S_L = 2.24\ \frac{\text{liters}}{\text{sec cm}}$

CONCLUSIONS

From the results presented it may be concluded that:

(1) The total charge stored in unit length of the rotating electron cloud is maximized if the inner turning point is near the anode, $Q(x_i)\big|_{max} \rightleftarrows x_i = X_i + \delta$, $\delta << 1$.

(2) The total charge stored in unit length increases as the electron Hamiltonian increases or as the ratio of outer cylinder radius to outer turning point radius decreases (which are equivalent).

(3) The total charge per unit length considered as a function of the anode radius exhibits a maximum and that this maximum is shifted toward larger anode radii as the Hamiltonian increases or as X_o decreases.

(4) The ion production rate considered as a function of anode radius exhibits a maximum but which does not coincide with the stored charge maximum.

(5) The ion production rate increases as the Hamiltonian increases or X_o decreases.

(6) The potential distribution modification resulting from the space charge insertion is a strong function of the anode radius, decreasing as X_i increases.

(7) The potential distribution modification resulting from the space charge insertion is only a weak function of X_o , increasing with X_o .

(8) The outer turning point kinetic energy is a strong function of anode radius, increasing with X_i .

(9) The orbit period, the electron mean velocity, and the minimum charge density are weak functions of both X_i and X_o .

(10) Maximum orbital stability corresponds to maximum space charge.

REFERENCES

1. Feakes, F.; Muly, E. C.; and Brock, F. J.: Extension of Gage Calibration Study In Extreme High Vacuum. (Oribtron and Magnetron Studies), NASw-1137, 1967.

2. Widder, D. V.: Advanced Calculus. Prentice-Hall Inc., Englewood Cliffs, New Jersey, 1961.